Hydrological Processes

WILEY

RESEARCH ARTICLE

The Influence of Geomorphology on Storage and Surface Water–Groundwater Interactions in Mountainous Headwater Streams

Zachary Perry[1] | Catalina Segura[1] | J. Renée Brooks[2] | Sadao Takaoka[3] | Frederick J. Swanson[4]

[1]Department of Forest Engineering, Resources, and Management, Oregon State University, Corvallis, Oregon, USA | [2]Department of Forest Ecosystems and Society, Oregon State University, Corvallis, Oregon, USA | [3]Department of Geography, Senshu University, Tokyo, Japan | [4]Pacific Northwest Research Station, United States Forest Service, Corvallis, Oregon, USA

Correspondence: Zachary Perry (zachary.perry@oregonstate.edu; perryz@oregonstate.edu)

Received: 16 July 2025 | **Revised:** 3 November 2025 | **Accepted:** 4 December 2025

Keywords: catchment hydrology | groundwater | hydrologic connectivity | Pacific northwest | rain-snow zone | volcanic terrain | water stable isotopes

ABSTRACT

We investigated the influence of landslide deposits on hydrologic connectivity and subsurface water movement in small headwater catchments in the Western Cascades, Oregon, USA. We examined isotopic variations in surface water across multiple catchments, comparing wet and dry periods to assess how antecedent moisture influences hydrologic connectivity and groundwater interactions. Seasonal shifts in $\delta^{18}O$ values reveal that hydrologic connectivity increases during wet conditions, resulting in more uniform isotopic signatures across catchments due to enhanced vertical and lateral water movement in the subsurface. In contrast, during dry periods there was greater spatial variability in $\delta^{18}O$, reflecting localised groundwater contributions and reduced connectivity. Notably, some catchments with high proportions of earthflow terrain maintain consistent water isotopic ratios across seasons, suggesting persistent groundwater inputs from landslide deposits. Spatial patterns in $\delta^{18}O$ also point to subsurface inter-catchment flow paths facilitated by landslide deposits. Streamflow measurements during the dry season further support these findings. Catchments underlain by older, stabilised landslide deposits had highly variable unit discharge and frequent periods of flow cessation, consistent with weaker subsurface connectivity and limited water retention. In contrast, catchments draining active earthflows maintained relatively high unit discharges and perennial flow, indicating stronger subsurface linkages and greater potential for water accumulation that sustains both flow and ongoing slope movement. We estimated storage potential within landslide deposits and then used this to estimate catchment storage potential. Catchment storage was negatively correlated to variability in isotopic ratios, indicating an inverse relationship between catchment storage and variability in water sources in both space and time. Overall, our results demonstrate that geomorphic setting—particularly the presence and structure of landslide deposits—can exert strong control on the spatial distribution of hydrologic connectivity in mountain catchments. These insights improve our understanding of how subsurface properties mediate water movement and streamflow resilience under varying climate conditions.

1 | Introduction

Headwater streams are critical to the preservation of aquatic ecosystems, making up around two thirds of total stream length in a given river network (Richardson 2020). They play a crucial role in maintaining biodiversity, providing a myriad of services to communities within small catchments and significantly influencing the larger river network (Finn et al. 2011; Golden et al. 2025). These streams influence downstream water availability, contribute nutrients along the river

network, and support interconnected aquatic communities across various stream sizes (Freeman et al. 2007). In headwaters of the Western United States, water supply largely relies on winter precipitation, as summer rainfall is minimal. Consequently, summer baseflow is sustained by water stored in subsurface layers and high-elevation snowpack. However, global warming has led to snowpack declines across the region (Mote et al. 2018), which in turn may alter subsurface storage and streamflow dynamics (Kalra et al. 2008; Siirila-Woodburn et al. 2021). These impacts are expected to be most pronounced in streams within the rain–snow transition zone, where rising temperatures are shifting the zone upslope. As a result, systems that historically received both rain and snow are increasingly becoming rain-dominated (Vano et al. 2015). Quantifying the consequences of these changes remains challenging, as water routing in mountainous terrain is governed by complex patterns of connectivity and variable subsurface storage.

Hydrologic connectivity–the degree to which water moves within lateral and vertical dimensions–plays a critical role in determining the interactions between groundwater and surface waters (Pringle 2001; Bracken and Croke 2007). Connectivity is influenced by geology (Pfister et al. 2017), topography (Tetzlaff et al. 2009; Jencso and McGlynn 2011), and climatic variability (Nippgen et al. 2011; Segura et al. 2019). Spatial variations in lithology and geomorphic history define the structural template for hydrologic pathways, influencing subsurface flow and storage capacity (Nippgen et al. 2011; Bracken et al. 2013). For instance, permeability, fracture networks, and soil properties determine how water moves vertically between surface and groundwater systems (Keller et al. 1988; Johnson, Christensen, et al. 2024), while topography and landscape gradients influence lateral flow paths (Tetzlaff et al. 2009; McGuire and McDonnell 2010; Xiao et al. 2019). Climatic variability further modulates connectivity, with precipitation form and pattern (Nippgen et al. 2015), storm intensity (Bracken and Croke 2007), and seasonal changes in snow (Segura 2021) determining the spatial extent and duration of surface and subsurface flow networks. For example, during wet periods, subsurface connections to surface water may strengthen as water tables rise, whereas droughts can weaken these links, isolating groundwater reserves from surface systems. Although substantial progress has been made in understanding the mechanisms of connectivity, the influence of spatial variability in geomorphology on regional connectivity remains poorly understood.

In mountainous regions such as the volcanic terrain of the Western Cascades, OR, USA, landslides of various types play a pivotal role in shaping the landscape (Swanson and James 1975). The term landslide broadly refers to a wide variety of soil and rock movements (Varnes 1978). In the Western Cascades, common types include debris slides, which are rapid movements of earth material down steep slopes, typically leaving behind a discernible headscarp. When this material enters and travels along a stream channel, it is referred to as a debris flow. Rotational slides are similar to debris slides but differ in that the material moves along a concave failure surface, producing a steep headscarp above a slump bench on the displaced material. Earthflows are slower, episodically moving landslides driven in part by seasonal cycles of precipitation (Pyles et al. 1987) and clay mineral expansion and contraction. Earthflow terrain typically occurs on moderate slopes and is characterised by complex surface topography and disrupted stream networks both on and around the perimeter of the deposit. These features can persist for millennia, cover large areas (often exceeding 1 km^2), and may transport intact forest vegetation on their surface (Swanson and Swanston 1977).

Landslides and their deposits are common in mountain landscapes, especially Oregon and similar tectonically-active zones with weak bedrock (Gómez et al. 2023), but their impact on hydrologic connectivity is not well characterised. Previous research demonstrated the hydrologic influence of landslide deposits on water storage potential (Weekes et al. 2014) in the Rocky Mountains in Colorado. However, the variability in storage and subsurface flow paths introduced by deposits of differing depths, ages, and extent remains poorly quantified. One study on earthflow deposits in the Western Cascades suggested that these features could store and release water over interannual timescales, impacting runoff generation and flow intermittency (Swanson and Swanston 1977). More recently, the influence of landslide deposits on baseflow sources was inferred from tracer information (Segura et al. 2019; Ortega et al. 2025). Modern advances in water tracers, catchment hydrology, and landscape analysis offer new opportunities to more rigorously investigate the role of landslide deposits in shaping hydrologic connectivity across spatial and temporal scales. Understanding these dynamics is crucial for predicting how small catchments will respond to climate variability.

Water stable isotopes (WSI) have become a central tool in hydrology to investigate subsurface water dynamics. WSI serve as natural tracers for fingerprinting water and studying hydrologic dynamics, with their spatial and temporal variability in streams aiding hydrologic investigations (Bowen et al. 2019; Jasechko 2019). Notably, WSI have been fundamental in the study of water transit times (see reviews by McGuire and McDonnell 2015; Benettin et al. 2022). In mountainous settings, WSI have been used extensively to understand the role of topography (McGuire et al. 2005; Mueller et al. 2013; Gao et al. 2021), the subsurface (Soulsby et al. 2015; Pfister et al. 2017; Zhang et al. 2019), and climate variability (Brooks et al. 2025; Penna et al. 2015; Segura 2021) in determining water storage and transit time. Relevant to this investigation, WSI have been used to understand water flow paths and contributing source areas (Rock and Mayer 2007; Brooks et al. 2012, 2025; Weekes et al. 2014; Nickolas et al. 2017; Ortega et al. 2025).

In this study, we investigate the influence of geomorphology on hydrologic connectivity dynamics by coupling WSI observations in precipitation and streams with landscape analyses and streamflow observations. We used a snapshot of spatial variations in specific discharge to contextualise WSI and infer subsurface water dynamics. Additionally, we investigated the occurrence of intermittent streamflow as it pertains to different landscape types. Specific discharge has been used extensively to characterise spatial variability in streamflow as a result of climate variability and changes in physiography (Shaman et al. 2004; Payn et al. 2012; Lyon et al. 2012; Asano et al. 2020). Lastly, we used digital elevation models (DEMs)

derived from Light Detection and Ranging (LiDAR) to characterise depth and extent of landslide deposits to tease out their role in subsurface water dynamics and hydrologic connectivity. LiDAR has been used to aid in hydrologic investigations in landscapes that are traditionally difficult to study due to topographic complexity (Hopkinson et al. 2009; Buchanan et al. 2014; Segura et al. 2019).

Untangling the relationship between geomorphology and subsurface water dynamics within heterogeneous landscapes is key to advancing our understanding of how regional and catchment-scale landscape features control hydrological processes. Our goal was to examine how landslide deposits influence water movement. These insights are critical for predicting future water availability in rain-snow transition zones, particularly under the pressures of a warming climate. This study has three main research questions:

1. How do landslide deposits modulate hydrologic connectivity and affect groundwater–surface water interactions under varying climatic conditions?
2. How do the extent and depth of landslide deposits influence the hydrologic connectivity within and between catchments at various spatial scales?
3. How does the spatial distribution of landslide deposits influence the occurrence of intermittent streams and spatial patterns in unit discharge?

2 | Methods

2.1 | Study Site

This study was conducted in the HJ Andrews Experimental Forest (hereafter Andrews Forest) located in the Western Cascades of Oregon (44.2° N, 122.25°W) (Figure 1a). Originally established in 1948, the Andrews Forest has been an NSF-funded Long Term Ecological Research (LTER) site since 1980. The site spans wide elevational (430–1631 m.a.s.l) and climatic gradients. The climate is Mediterranean, with dry summers and wet winters. Annual precipitation varies with elevation from 2300 mm to > 3550 mm, with ~80% of the annual precipitation falling between November and May. In general, snowpack persists from mid-November until the end of June above 1000 m.a.s.l. Below this elevation, snowpack rarely persists for more than 2 weeks (Jennings and Jones 2015; Jones and Perkins 2010). Vegetation is primarily old-growth coniferous forest (75% of the area) dominated by Douglas-fir (*Pseudotsuga menziesii*) and western hemlock (*Tsuga*

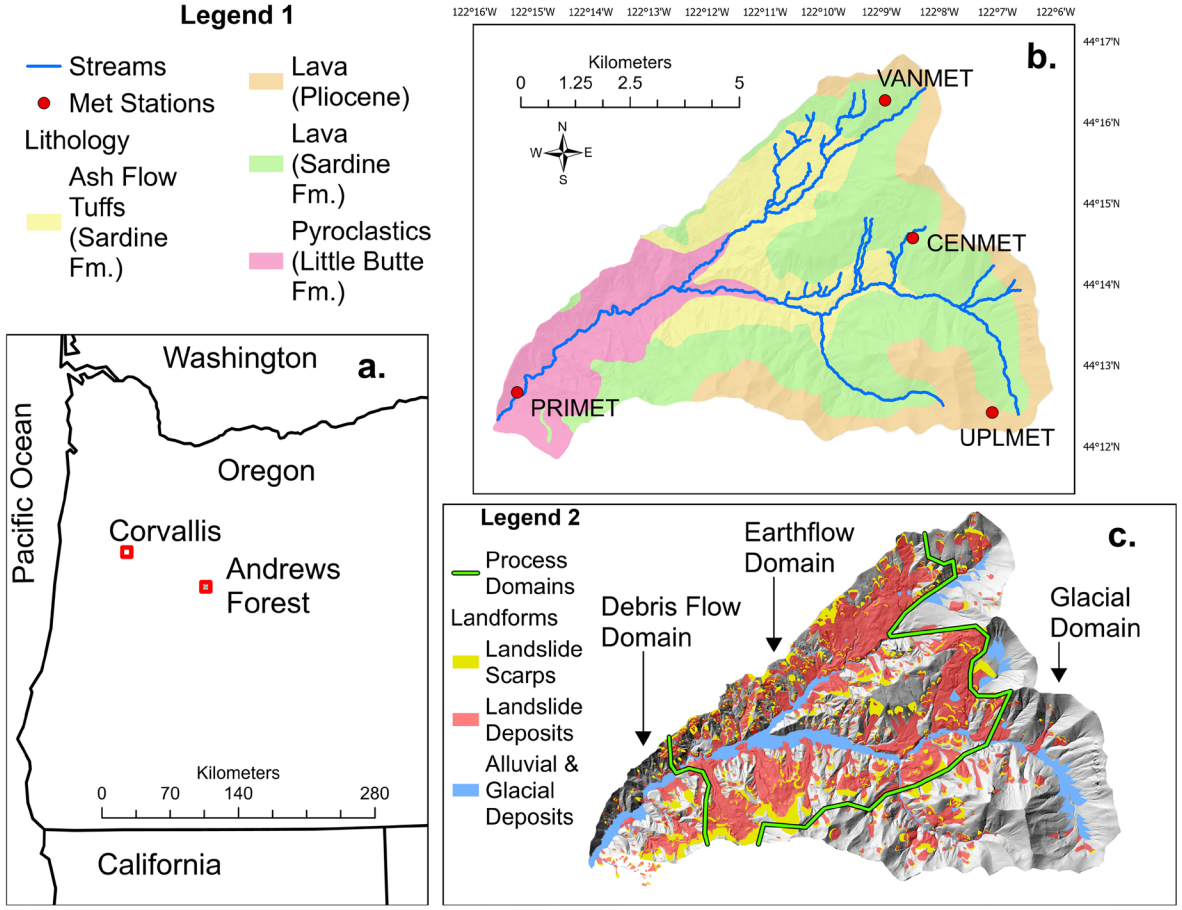

FIGURE 1 | Site map of the Andrews Forest. (a) Location of the Andrews Forest and Corvallis within Oregon, USA. (b) Lithology in the Andrews Forest and long-term meteorological stations (red circles). (c) Geomorphology map of the Andrews Forest, highlighting the locations of landslide, glacial, and alluvial deposits, along with landslide scarps (adapted from map created by S. Takaoka & FJ Swanson). The three process domains (Goodman et al. 2022) are delineated, and are based on the overarching geomorphologic processes.

heterophylla) at lower elevations and by noble fir (*Abies procera*) and Pacific silver fir (*Abies amabilis*) at upper elevations. The area is underlain by volcanic rock, stratified into three geologic zones (Figure 1b). Ridges are underlain by Miocene lava flows, which have relatively high porosity, while lower elevation areas are underlain by ash flow and air fall tuffs, and alluvial tuffaceous sedimentary rocks (Swanson 2013; Walker and MacLeod 1991). The landscape is spatially heterogenous, with influence from glacial, landslide, and fluvial processes (Figure 1c). Upper Lookout Creek drains U-shaped valleys, a relic of glacial erosion. The McRae Creek drainage and portions of Upper Lookout drain earthflow terrain, shaped by landslides of various types (Swanson and James 1975). As such, the region can be divided into three process domains: debris flow-, earthflow-, and glacially dominated geomorphologies (Goodman et al. 2022). In general, soils are loamy, have high infiltration capacity, and are well drained due to high porosity and large pore sizes in addition to a relatively high gravel content (Dyrness 1969; Rothacher et al. 1967; Hawk and Dyrness 1972).

2.2 | Experimental Design

To investigate the relationship between landslide deposits and hydrologic connectivity, we selected 12 headwater catchments within two adjacent 4th order catchments (Figure 2) that spanned earthflow and glacially dominated landscapes (Figure 1). These catchments represent a range of physiographic conditions, and importantly, a range of influences from landslide deposits (Table S1). Within these systems, we conducted synoptic sampling campaigns for water stable isotopes (WSI) during wet and dry periods to cover a range of hydrologic conditions (Section 2.3). We characterised the regional isotopic lapse rate and analysed stream WSI data in the context of expected regional precipitation processes to understand groundwater dynamics (Section 2.5). Additionally, we measured unit discharge and flow intermittency during a single dry period to characterise spatial variability in flow conditions (Section 2.6). We quantified landslide deposit depth and extent using LiDAR data to estimate landslide deposit volume per catchment (Section 2.7). Finally, we used the standard deviation of $\delta^{18}O$ as a proxy measure of hydrologic connectivity and related this to landslide storage to understand the role these deposits play in regulating water movement and catchment storage (Section 2.8).

The synoptic sampling campaigns were ranked 1–4 based on their relative wetness considering climatic conditions (Table 1). Campaigns in May 2022 and May 2023 were considered 'wet' conditions. Conversely, the campaigns in August 2021 and August 2022 represent 'dry' conditions, with August 2021 being drier than August 2022, based on precipitation and streamflow data (Figure S1) (Daly et al. 2024; Johnson, Wondzell, and Rothacher 2024). Conditions in May 2022 were wetter than in May 2023 despite the higher snow accumulation in 2023. Cumulative precipitation was lower in 2023, with much of the wet season precipitation falling as snow. Mean annual precipitation across the 20-year record was 2420 mm. Annual precipitation for water years 2021, 2022, and 2023 was 2211, 2628 and 2089 mm, respectively. We selected May and August to capture the high-flow snowmelt period and the low-flow groundwater dominated period, respectively, but the years also added significant variation to the hydrologic condition.

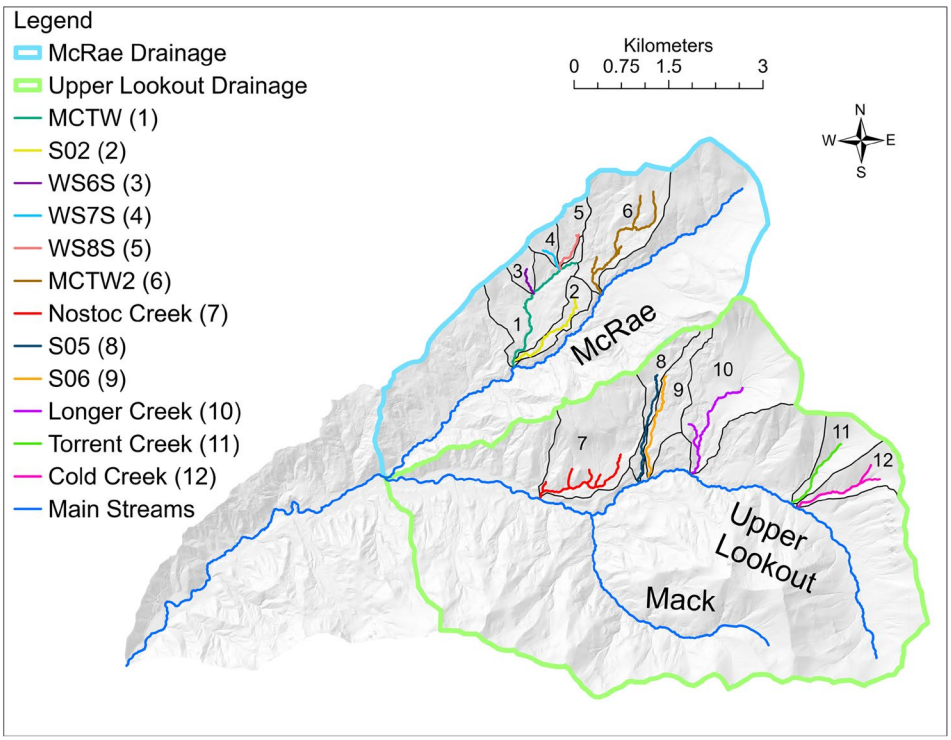

FIGURE 2 | Map of the study streams in the Andrews Forest. Primary streams are shown in blue and the 12 headwater streams we investigated are depicted in various colours. The number in the legend corresponds to the number shown on the map for each study stream. Upper Lookout and McRae Creek drainages are highlighted, as well.

TABLE 1 | Summary of hydrologic conditions during each sampling campaign, based on the analysis of meteorological and hydrological data (Figure S1) from stations in the Andrews Forest (Figure 1).

Sampling campaign	Hydrologic conditions	Wetness rank
August 2021	Summer sampling following a relatively dry winter. Flows were lower than average, with streamflow becoming intermittent in multiple study streams.[a]	4
May 2022	Spring sampling at the tail end of the snow melt. Based on soil moisture and flow records, this was the wettest sampling campaign.	1
August 2022	Summer sampling following a wet winter. Flows were higher than average, though baseflow conditions still presented intermittent flow in some streams.	3
May 2023	Spring sampling at the tail end of the snow melt. Maximum snowpack levels were highest of all sampling periods, though below average rainfall led to below average flow.	2

Note: Wetness was ranked (4 = driest conditions, 1 = wettest conditions) to differentiate the campaigns.
[a]MCTW2, WS8S, WS7S, WS6S, S05.

2.3 | Water Sampling for Stable Isotope Ratios

Stream water samples were collected across the 12 headwater catchments (1st–3rd order) during the four synoptic campaigns. We also sampled the main stems of Lookout and McRae Creeks (4th order) during baseflow conditions in August (Figure 2 and Table S1), for a total of 14 study catchments. During the dry campaigns (August), we covered the full extent of flowing water in each stream. Conversely, in wet campaigns (May), we sampled shorter portions of some streams given logistical constraints. Sampling campaigns were conducted over 2–5 days. In 1st–3rd order streams, samples were collected at a 50 m interval, and in 4th order streams at a 100 m interval. All samples were georeferenced using Avenza Maps Pro, with an accuracy of ~±5 m on GPS enabled smart devices.

Weekly composite precipitation samples were collected between 2015 and 2023 at the PRIMET meteorological station (430 m, Figure 1) (Segura et al. 2025) and at Corvallis EPA Pacific Ecological Systems Division climate station (Brooks et al. 2012, 2025). In both locations, we used PALMEX integrating rain samplers that meet International Atomic Energy Agency (IAEA) recommendations to prevent evaporation (Gröning et al. 2012). All water samples were collected and stored in 20 mL high density polyethylene or borosilicate glass vials with conical inserts in the cap to prevent evaporation during storage. All stream samples and Andrews Forest precipitation samples were analysed in the Watershed Processes Laboratory at Oregon State University. All Corvallis precipitation samples were analysed at the Integrated Stable Isotope Research Facility (ISIRF) at United States EPA Pacific Ecological Systems Division in Corvallis, Oregon.

2.4 | Laboratory Methods

At the OSU Water Processes Laboratory, water stable isotope ratios were measured in a total of 1246 stream water samples and 317 precipitation samples using a cavity ring down spectroscopy liquid and vapour isotopic measurement analyser (Picarro L2130-i, Picarro Inc., CA). Two internal standards were used to develop calibration equations, and a third standard was used to assess accuracy. All the standards were calibrated against the IAEA primary standards for Vienna Standard Mean Ocean Water (VSMOW), Standard Light Antarctic Precipitation, and Greenland Ice Sheet Precipitation. Precision was 0.02‰ and 0.09‰ for $\delta^{18}O$ and $\delta^{2}H$, respectively, based on the comparison of 102 duplicated samples. Accuracy was 0.01‰ ± 0.04‰ and 0.08‰ ± 0.25‰ for $\delta^{18}O$ and $\delta^{2}H$, respectively. Analytical methods for ISIRF are given in Brooks et al. (2025). Isotope values were reported in parts per thousand (‰) deviation relative to VSMOW (Craig 1961). Here, we use the terms isotopically higher or lower to indicate an increase or decrease in relative ^{18}O content of a sample. Mean volume-weighted precipitation values for $\delta^{18}O$ and $\delta^{2}H$ were calculated, but given the strong correlation between $\delta^{18}O$ and $\delta^{2}H$ (Figure S2), only $\delta^{18}O$ was used in the analysis.

2.5 | Isotopic Lapse Rate Estimation

We used surface water samples and volume–weighted precipitation samples to estimate a lapse rate for the Andrews Forest. For surface water samples, we calculated the mean isotopic ratio at the outlet of each catchment across sampling campaigns. This provided 14 mean isotopic ratio values from 14 streams with mean catchment elevations between 846 and 1283 m. For precipitation samples, we used the mean annual volume-weighted isotope ratios at PRIMET (460 m) and Corvallis (72 m) between the water years 2015 and 2023. We calculated the overall mean isotope ratio at each site by averaging over the 8-year record. We then used linear regression to calculate the relationship between isotopic ratios and elevation using both precipitation sites and the 14 stream sites.

The relationship between elevation and $\delta^{18}O$ was used to estimate the expected $\delta^{18}O$ at each study catchment outlet, based on their mean catchment elevations. By comparing these expected ratios to the observed values, we determined whether streams were isotopically lower, higher, or within the expected range given their elevation. Streams with lower isotopic values indicate catchments that are recharged with water received at higher elevations in the landscape. Streams with higher isotopic values indicate catchments that could be losing high elevation water through inter-catchment subsurface flow paths. We used this technique to infer subsurface water movement out of or into catchments.

2.6 | Streamflow Measurements and Flow Intermittency

Site-wide variability in unit discharge during baseflow conditions was estimated based on measurements of flow at stream-crossing culverts across the Andrews Forest during the summer of 2023 using a bucket and a stopwatch. We recorded observations of flow conditions (either dry or flowing) and took measurements where the culvert design allowed for it. For dry culverts, we visually confirmed the lack of flow both above and below the road. We believe that bypass of these culverts by flow through the fill is minimal due to the construction standards used to guarantee fill slope stability. Additionally, fine sediment deposition in the substrate at the head of the culverts serves to minimise culvert bypass. We visited 50 culverts during two surveys in August. Three measurements were taken at each culvert to estimate an average discharge. In addition to the bucket flow measurements, we compiled discharge during these days for seven experimental catchments in the Andrews Forest (Johnson, Wondzell, and Rothacher 2024) that drain into Lookout Creek. We also considered streamflow at Longer and Cold Creeks based on existing rating curves (Ortega et al. 2025). While we intended to characterise site-wide variability in unit discharge over the course of a few months, the outbreak of the Lookout Fire on August 5, 2023, halted data collection. Although this introduces a limitation to our study, we believe that our observations represent typical baseflow behaviour in terms of the relative differences between sites.

2.7 | Landscape Characterisation With LiDAR

Landform units were identified by interpretation of the shaded maps generated from the 1-m LiDAR DEM and subsequently mapped as polygons using GIS. In the GIS-based landform mapping process, the landform classes were identified and delineated by superimposing contour lines at 2-m intervals generated from the DEM on to the shaded map in order to facilitate the identification of topographic features. For the landslide landforms, the protocol developed by Burns and Madin (2009) was referenced to map the extent of landslide scarps and landslide deposits, noting the presence of micro landforms, such as scarps, deposits, and altered streams (Varnes 1978). The morphological characteristics of landslide landforms reported in previous studies from this region were also taken into consideration (Swanson and James 1975; Swanson and Swanston 1977). Alluvial landforms that develop along streams include floodplains, river terraces, and alluvial fans. Glacial landforms such as U-shaped valleys and cirque valleys are present in the upper reaches, and some of the sedimentary landforms on the valley floor are considered to be of glacial origin.

To characterise the potential water storage capacity of landslide deposits, estimates of deposit depth were calculated based on DEM derived surface elevation measurements. We measured the depth of stream channel incision (where available) and the height of deposit toes on terraces and streambanks. Based on the degree of weathering of the larger deposits, the presence of Mazama volcanic ash (~7700-years old), the presence of 500-year-old forests, and detailed observations of individual features, the relative age of these deposits has been determined and likely span a period since the beginning of the Holocene (Swanson and James 1975). In particular, older deposits are common in the McRae Creek drainage, while some of those along Upper Lookout Creek are younger. Fluvial erosion has carved deep stream channels through and along the margins of various landforms, allowing for a minimum estimate of deposit thickness. Additionally, the height of the toes of some earthflow deposits provided minimum estimates of their thickness. Elevation profiles were captured approximately every 100 m along streams and landslide deposit margins and an average value of streamflow incision and/or deposit toe height was used to characterise individual deposit depths (Figures S3 and S4). We grouped deposits within 6 distinct landforms based on the largest landslide deposits in each region (Figure S4). While topographic variability within these landforms can be high, using a single representative mean value for landform depth provides our best estimate of deposit thickness, acknowledging that local variability in depth is not fully captured. We estimated deposit porosity using a range of values found in the literature for landslide deposits. These estimates ranged from 25%–40% porosity (Malet et al. 2004; Nereson et al. 2018; Zhang et al. 2024). We then calculated a potential range of subsurface water storage (m^3) for each deposit of interest using Equation (1).

$$\text{Potential Storage} = \text{Deposit Thickness} * \text{Porosity} * \text{Deposit Area} \quad (1)$$

All spatial and landscape analyses were performed using ArcGIS geographical information system (GIS) software (Version 3.2.0). We used a 1-m DEM developed using aerial LiDAR, acquired in 2020 (OCM Partners 2025).

2.8 | Catchment Landslide Storage and Predicted Variability in $\delta^{18}O$

We used estimates of deposit storage to estimate maximum catchment landslide storage based on the percentage of land area underlain by deposits (Table S1) using Equation (2). Catchment topographic boundaries were delineated manually in ArcGIS using a 5 m contour and used to extract the percentage of each underlain by landslide deposits. For estimates using Equation (2), we used the upper range of porosity values (40%). We assumed a single value for the depth of deposits for each catchment.

$$\begin{aligned}\text{Catchment Landslide Storage} = {} & \text{Drainage Area } (m^2) \\ & * \text{Area Underlain by Deposits } (\%) \\ & * \text{Depth of deposits (m)} * \text{Porosity } (\%)\end{aligned} \quad (2)$$

We then created a linear regression model to relate estimates of catchment landslide storage to standard deviation in $\delta^{18}O$ for catchments in the earthflow-dominated process domain. Here, we use standard deviation in $\delta^{18}O$ as a proxy measurement of hydrologic connectivity, where low variability across samplings would indicate consistent groundwater contributions, and vice versa.

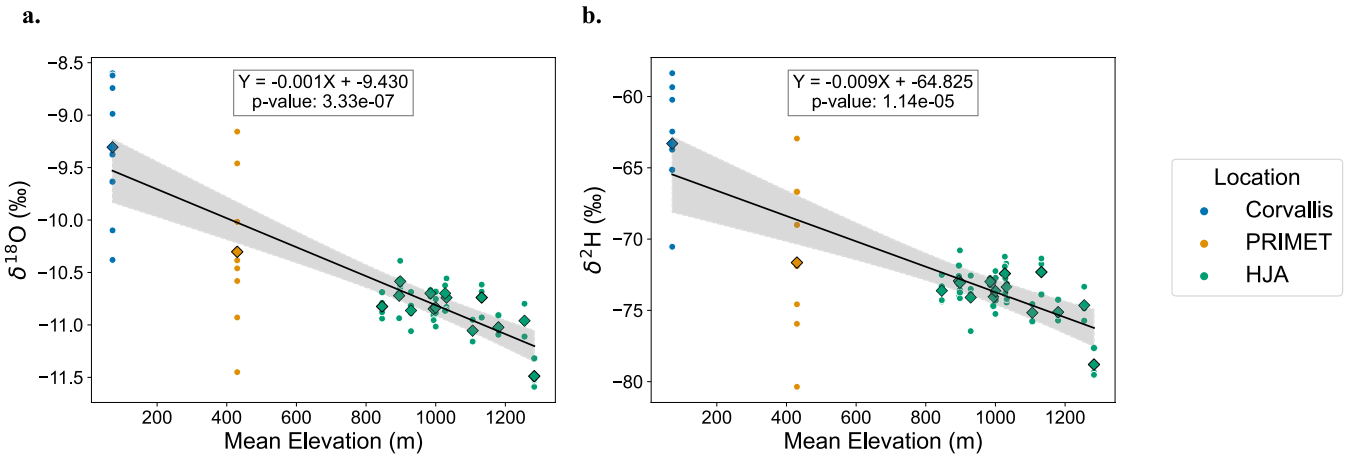

FIGURE 3 | $\delta^{18}O$ (‰) (a) and $\delta^{2}H$ (‰) (b) plotted against mean elevation for 2 precipitation sites (Corvallis & PRIMET) (2015–2022) and 14 stream sampling sites in the Andrews Forest (2021–2023). The circles represent: In precipitation—the mean volume weighted values for each water year in the record, in streams—the mean value for each of the 5 campaigns, per site. The diamonds represent the overall mean value for each site. The linear regression was calculated using the overall mean values (95% CI $\delta^{18}O$: −0.002 to −0.001, $\delta^{2}H$: −0.012 to −0.007).

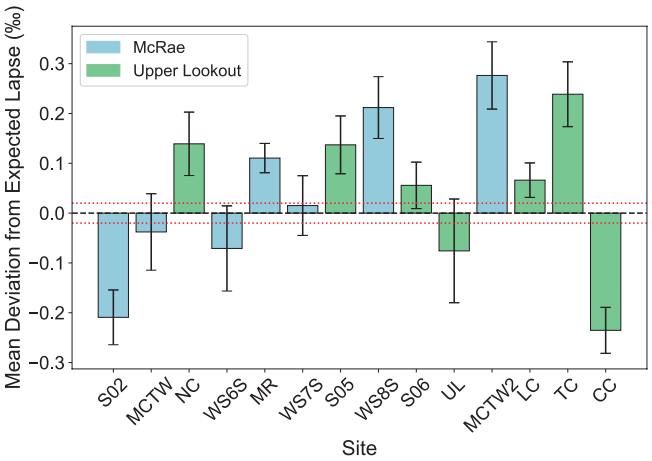

FIGURE 4 | Average deviation in $\delta^{18}O$ (‰) from expected lapse at each site. These values represent the mean deviation across all sampling campaigns. The dotted red lines show the Picarro Analyser precision (±0.04) based on 102 duplicate samples to highlight results that are significant. The error bars associated with each bar represent the standard error of the mean. Values above zero represent sites that are measuring higher $\delta^{18}O$ than expected and values below zero represent sites that are measuring lower $\delta^{18}O$ than expected. Sites are ordered by ascending mean catchment elevation.

3 | Results

3.1 | Isotopic Rainout Effect and Deviations From Expected Lapse

The mean regional lapse rate considering isotope data from Corvallis and the Andrews Forest was −0.15‰ ± 0.000/100 m for $\delta^{18}O$ and −0.96‰ ± 0.001/100 m for $\delta^{2}H$ (Figure 3). Using this regional lapse relationship, we compared the observed mean $\delta^{18}O$ at each catchment outlet to its expected value, based on the mean catchment elevation (Figure 4). We found that for the 4th order streams, mean $\delta^{18}O$ values in Upper Lookout Creek (UL) were lower than the lapse rate would predict by 0.09‰ and in McRae Creek (MR) mean $\delta^{18}O$ values were higher by 0.08‰. Smaller tributaries within these two drainages were both higher and lower than predicted by the lapse rate. Mean $\delta^{18}O$ values were lower (−0.06‰ to −0.25‰) than predicted in Cold Creek (CC), S02, MCTW, and WS6S while mean $\delta^{18}O$ values in Torrent Creek (TC), Longer Creek (LC), MCTW2, NC, S05, S06, and WS8S were higher than expected (0.06‰–0.27‰). Mean $\delta^{18}O$ values in WS7S did not significantly deviate from the expected lapse based on the precision of the measurement.

3.2 | $\delta^{18}O$ of Stream Water

The range of $\delta^{18}O$ over the entire sample period was −9.91 to −11.74‰ but varied between synoptic sampling campaigns (Figure 5). Interestingly, the mean $\delta^{18}O$ differed the most between May samplings. May 2022 had the highest mean $\delta^{18}O$ at −10.81‰ and May 2023 had the lowest mean at −11.00‰. Meanwhile, August 2021 had a mean of −10.91‰ and August 2022 had a mean of −10.87‰. Differences in mean $\delta^{18}O$ between all samplings were significant, despite these differences being small (Table S2). This pattern, with May 2022 $\delta^{18}O$ values being the highest and May 2023 $\delta^{18}O$ values being the lowest, was also seen in individual streams (Table S3) with exceptions of 5 streams (LC, NC, S02, WS6S, WS7S) when August 2021 $\delta^{18}O$ values were the lowest observed.

Overall inter-stream $\delta^{18}O$ variability was higher in Upper Lookout compared to streams in McRae (Figure 5 & Table S4), but generally, stream $\delta^{18}O$ decreased with increasing elevation. In Upper Lookout, Cold Creek $\delta^{18}O$ was consistently and significantly lower ($\bar{\delta}^{18}0 = -11.45$‰) than all other streams (Figure S5) including the adjacent Torrent Creek, though the mean elevations differ by only 28 m. In another example of adjacent streams, S05 had consistently higher $\delta^{18}O$ values when compared with S06 ($\bar{\delta}^{18}0 = -10.72$‰ vs. $\bar{\delta}^{18}0 = -10.89$‰) even though their mean catchment elevation is only 37 m apart. In the McRae Creek drainage, isotopic ratios were spatially more homogenous, though still exhibiting unique trends. Despite draining the catchment with lowest mean elevation (Table S1), S02 ($\bar{\delta}^{18}0 = -10.85$) had the second lowest $\delta^{18}O$ in the McRae

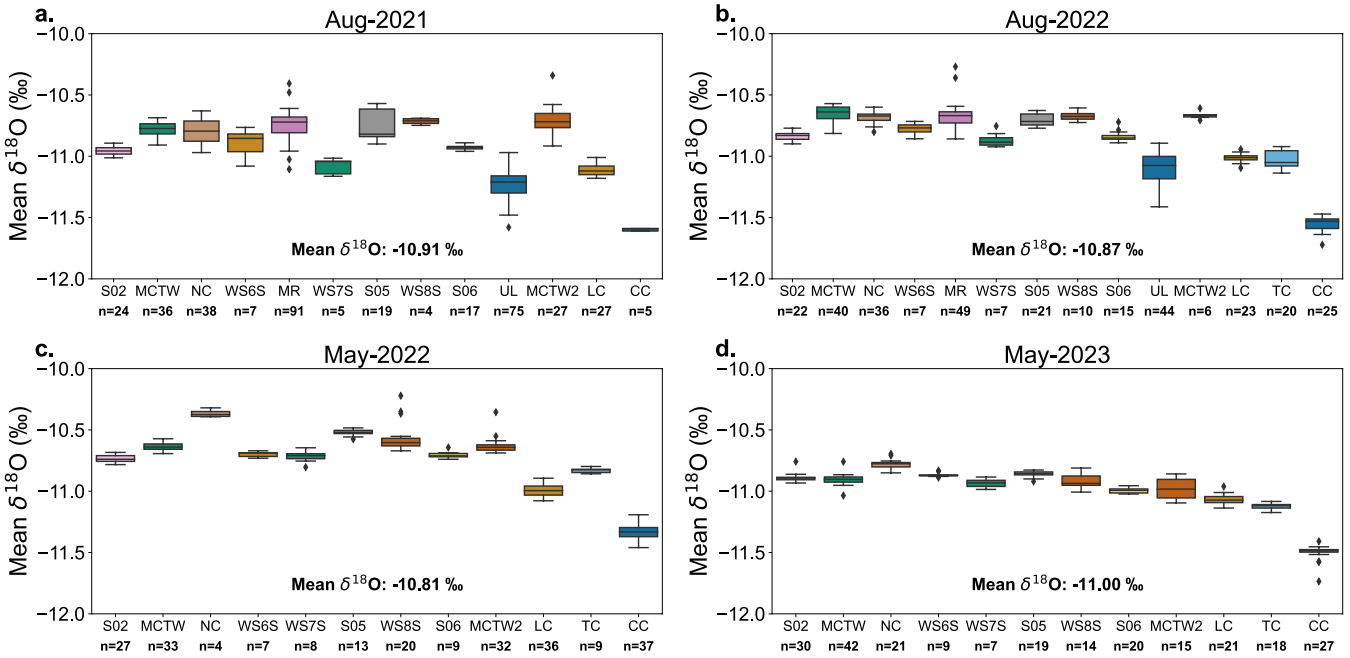

FIGURE 5 | Distribution of $\delta^{18}O$ (‰) in each stream sampled across four synoptic campaigns (a) August 2021, (b) August 2022, (c) May 2022, (d) May 2023. Boxes depict the median (line) and the interquartile range (25%–75%). Whiskers represent 1.5× the interquartile range. The number of samples collected per site is indicated below the site name. Sites are ordered by ascending mean watershed elevation (Table S1).

Creek drainage. WS8S had a higher mean isotopic ratio ($\bar{\delta}^{18}0 = -10.70$) than WS7S ($\bar{\delta}^{18}0 = -10.88$) despite WS8S being higher in mean elevation by 27 m. Lastly, MCTW2 and MCTW had isotopically similar $\delta^{18}O$ values ($\bar{\delta}^{18}0 = -10.73$ vs. $\bar{\delta}^{18}0 = -10.75$) despite MCTW2 draining a catchment with mean elevation 237 m higher than MCTW.

Based on the regional lapse rate (Figure 3), we expected a change of approximately −0.15‰ in $\delta^{18}O$ per 100 m of increasing elevation within a stream; however, this pattern was seldom observed. Longitudinal isotope profiles revealed that $\delta^{18}O$–elevation relationships were often weak or non-significant, and only a subset of sites exhibited statistically meaningful lapse rates (Figure 6, Table S5). On average across sampling campaigns, the most consistent and least variable lapse rates occurred in Cold Creek, Longer Creek, S06, and S02, though these relationships were often not significant. In contrast, WS6S, MCTW2, S05, WS7S, and WS8S showed greater variability among campaigns, with slopes occasionally significant but inconsistent in direction. Inter-stream variability in lapse rates was highest during August 2021, the driest sampling period. With the exception of WS7S and MCTW2, mean lapse rates across catchments were an order of magnitude smaller than the regional lapse rate. We assessed the variability of sample points along the longitudinal lapse profiles to infer the influence of tributary streams and the influence of groundwater recharge along stream reaches.

In the August campaigns, we noted significant and abrupt shifts in $\delta^{18}O$ values along the profile, deviating from the expected decrease with increasing elevation (Figure 6 boxes). This was particularly the case in Nostoc Creek, Longer Creek, WS6S, MCTW, Torrent Creek, and S05. In the cases of Longer Creek, MCTW, and Nostoc Creek, we attributed these abrupt shifts to the influence of tributaries entering roughly 115, 140, and 90 m of elevation above the confluence, respectively. In contrast, the shifts we observed in S05, TC, WS6S, and Longer Creek at roughly 115, 75, 25, and 65 m of elevation above the confluence, respectively, did not relate to the confluence of any tributary. This suggests the presence of high groundwater inflows. In Cold Creek, S02, and S06, longitudinal profiles between $\delta^{18}O$ and elevation were relatively flat, indicating relatively small changes in water sources moving along the stream. Indeed, the lack of decreasing $\delta^{18}O$ in Cold Creek indicates the influence of a known groundwater outflow which dominates streamflow in this creek (Segura et al. 2019; Ortega et al. 2025).

3.3 | Characterisation of Flow Regimes

We found evidence of intermittent streamflow during summer baseflow conditions in the Andrews Forest. Of the 50 culverts visited during the two streamflow surveys in August 2023, 64% (32 culverts) were dry (Figure 7). Only 3 of the 17 culverts visited in the McRae Creek drainage were flowing. In total, discharge was measured in 15 of the 18 culverts where flow was observed. In the remaining 3 culverts that had flow, discharge measurements were not possible. These discharge measurements together with discharge observations in Longer and Cold Creeks (Ortega et al. 2025), 8 experimental catchments, and the USGS gage station (no. 14161500) at the Lookout Creek outlet varied in unit discharge between 0.062 and 7.16 mm/day on August 1 (Figure 8a). Longer Creek, Cold Creek, and culvert C4 had the highest unit discharge, with Cold Creek having roughly twice the unit discharge of Longer Creek and over 14× the unit discharge of Lookout Creek at the outlet.

Unit discharge was higher in culverts within the Upper Lookout Creek drainage (C1–10) when compared to those measured in the

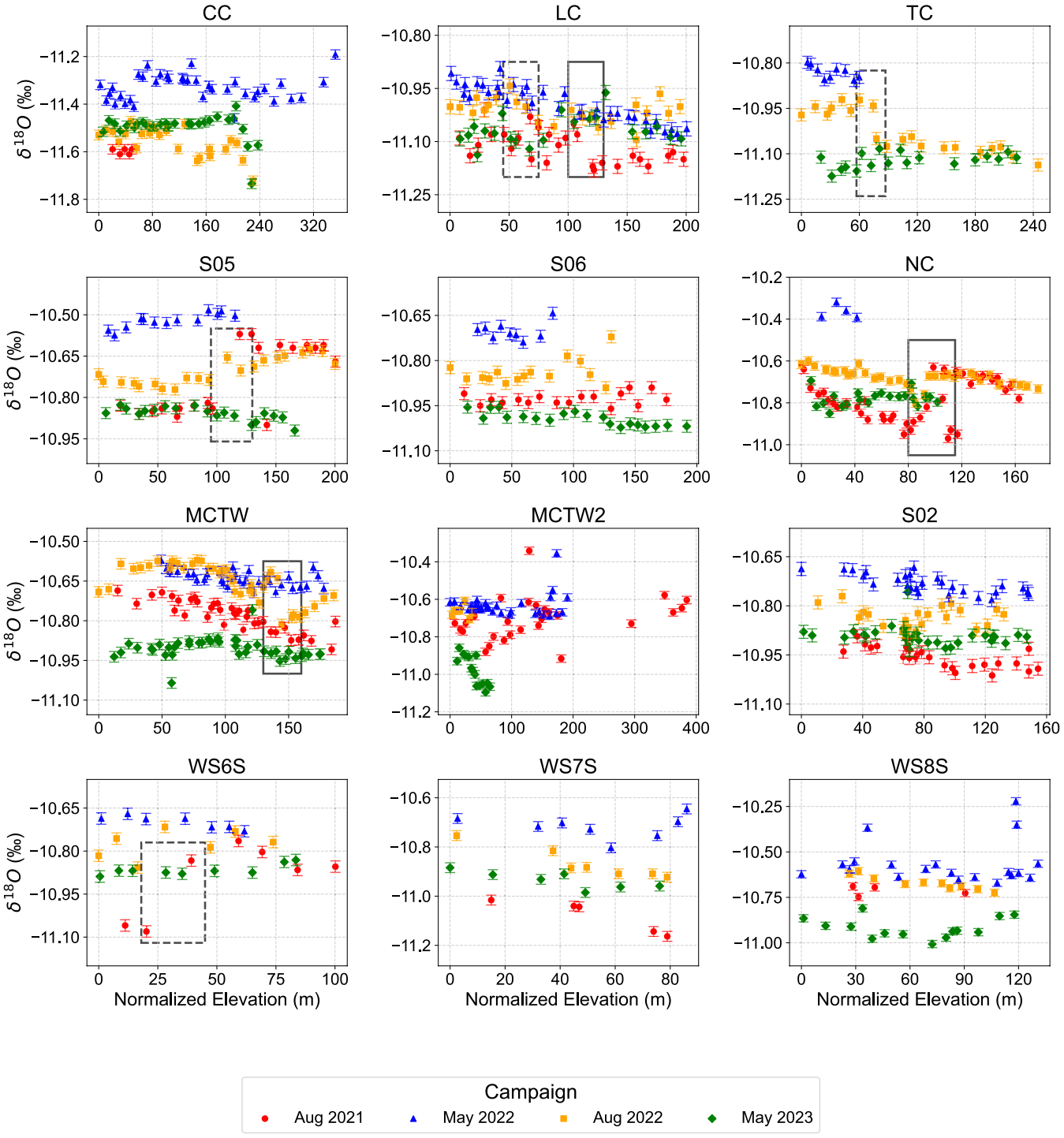

FIGURE 6 | Longitudinal profiles of $\delta^{18}O$ (‰) for each of the study streams along the elevational profile. Elevation corresponds to the elevation of the sampling location, normalised so that the stream's confluence represents an elevation of 0 m. Error bars represent Picarro Analyser precision in $\delta^{18}O$ (±0.04) based on 102 duplicates. Boxes on figures represent significant shifts in $\delta^{18}O$ (solid: Tributary influence, dashed: Groundwater influence). Sample elevation changes linearly with upstream elevation for all sites ($R^2 > 0.95$) except LC ($R^2 = 0.80$), where we observed relatively small changes in mean upstream elevation between some sampling points.

McRae Creek drainage (C11–15). Of note, a culvert in S06 (C6) had ~6× more unit discharge than an adjacent culvert in S05 (C7). Above the confluence of S05 with Upper Lookout Creek (C3), unit discharge increases to ~6× the unit discharge at the upstream culvert (C7). This change in flow coincides with the isotope shift along S05 during August between C7 and C3 (Figure 6). The high unit discharge observed in C4 and C6 in S06 corresponds to drainages that come out of a large active earthflow. The spatial distribution of dry culverts showed a higher proportion of dry streams in drainages along McRae Creek and in the lower portion of the Upper Lookout drainage (Figure 7). Overall, drainage area was a poor predictor of discharge due to the high level of variability (Figure 8b). This was particularly the case for the culverts (R^2: 0.22, p-value: 0.07), whereas in the experimental gauges

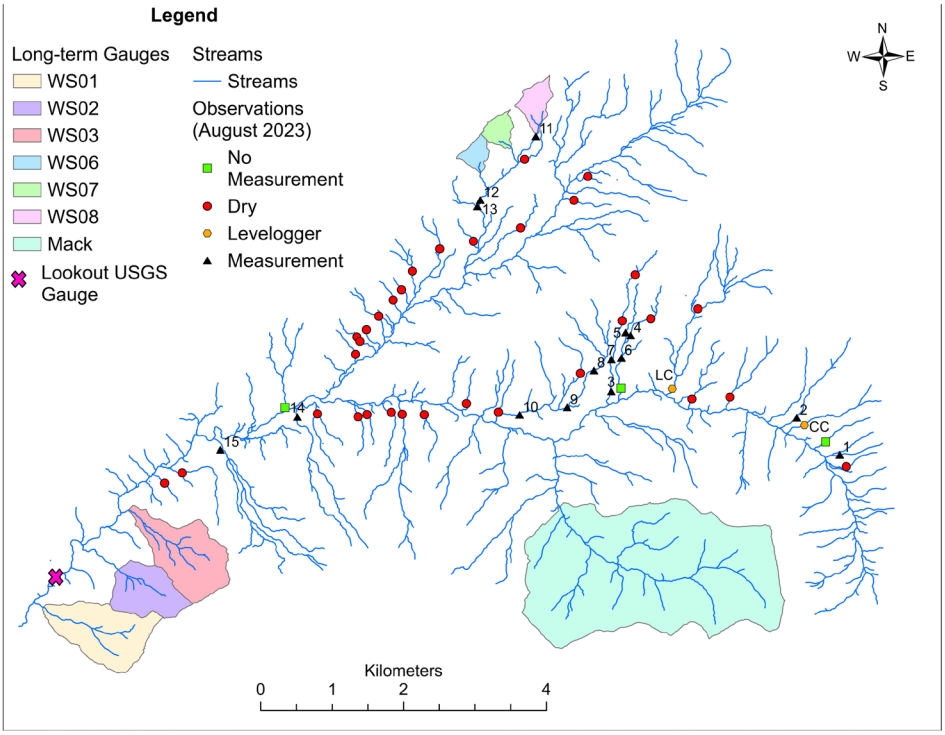

FIGURE 7 | Map showing locations of culverts visited during discharge surveys on 8/1/2023 and 8/8/2023. Red points represent culverts that were dry. Green points represent culverts with flow, but where a measurement was not possible. Black triangles represent culverts where measurements were taken, and the associated culvert ID is shown. Orange circles represent leveloggers installed in Cold Creek (CC) and Longer Creek (LC). Long-term stream gauges are represented by gauged watershed boundaries, with the exception of the USGS gauge on Lookout Creek (pink X).

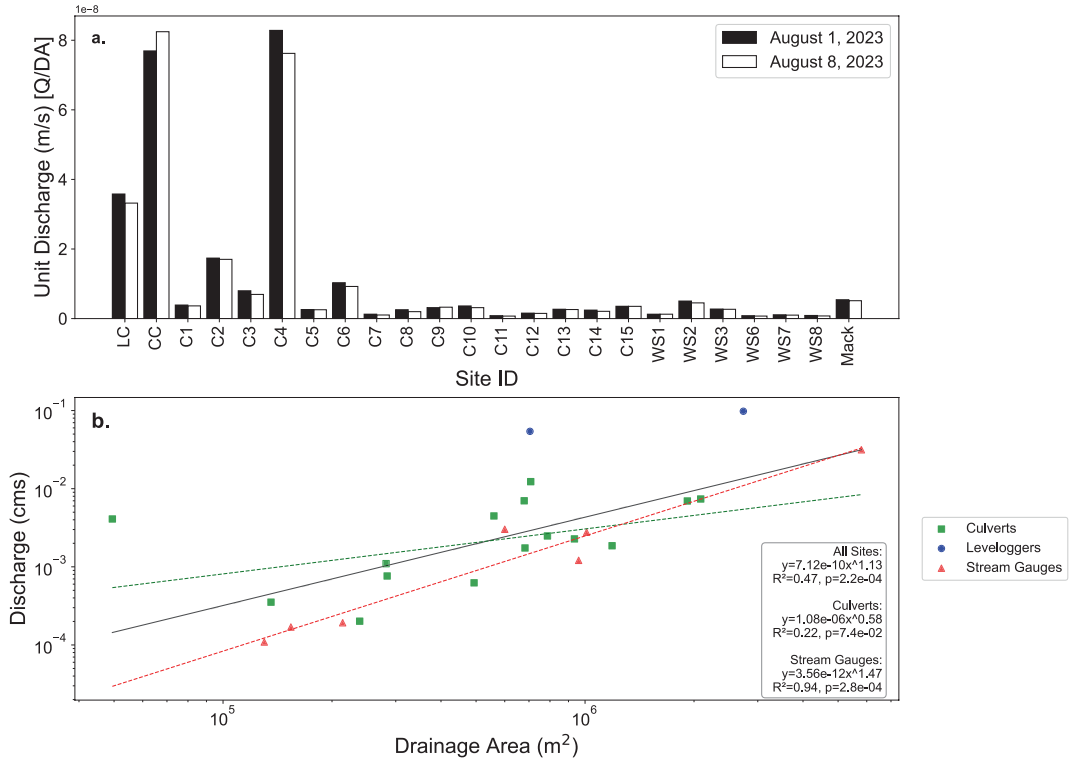

FIGURE 8 | (a) Unit discharge (Q/DA) readings from bucket and stopwatch surveys at culverts across the Andrews Forest. Measurements were completed during two separate surveys in August 2023. C# represents culvert sites where measurements were taken. LC and CC discharge values were obtained from stage readings and prior rating curves calculated at each site. WS01-WS08 and Mack Creek discharge data were obtained from the long-term stream gauges at the Andrews Forest and Lookout Creek data was obtained from the USGS (#14161500). (b) Discharge (cm) plotted against drainage area (m^2) from August 1, 2023, in a log–log scatter plot.

alone, drainage area was a strong predictor of discharge (R^2: 0.94, p-value: 0.03). Interestingly, we found that there was a statistical difference between drainage areas when comparing the group of culverts that had flow to the ones that were dry. We found that on average, culverts with flow drained larger catchments (Figure S6).

3.4 | Deposit Thickness and the Landscape's Influence on Isotopic Variability

Estimates of deposit thickness range from 4.2 to 23.5 m for six landforms located in both the McRae and Upper Lookout drainages (Figure 9 and Table S6). These estimates represent minimum approximations because channels may not be cut completely through the deposits to underlying bedrock. Using estimates of deposit thickness, porosity values of 25% and 40%, and Equation (1), we calculated the range of potential water storage in each feature. The overall range was from 3.2×10^5 to $1.2\times10^7\,m^3$ (Table 2). Considering the well-draining soils with high infiltration capacity (Dyrness 1969) in a landscape in which overland flow is very rare (Harr 1976), full saturation in soil and deposits is likely never achieved. As such, the storage estimates represent the theoretical maxima.

Estimates of catchment landslide storage in deposits ranged from ~4×10^4 to $9.8\times10^6\,m^3$ (Table S7). We used estimates of maximum catchment storage in landslide deposits to explain variability in mean catchment $\delta^{18}O$ (Figure 10 and Table 3). Linear regression results indicated that estimated maximum catchment storage in landslide deposits (Max Storage) was an effective predictor for Std Dev in $\delta^{18}O$ (R^2: 0.6, p-value: 0.014). Results indicate that as maximum landslide storage increases, isotopic variability in surface waters decreases. We performed this regression for all catchments within the earthflow-dominated process domain, with the exception of MCTW. Catchment storage in deposits is difficult to quantify in MCTW due to the size of the catchment and the range of landslide deposit depths. While we included this point on the figure, we left it out of the regression model because it is a significant outlier with a high degree of uncertainty in the storage prediction.

4 | Discussion

4.1 | Seasonal Fluctuations in Hydrologic Connectivity

The observed seasonal variability in isotopic ratios underscores the influence of antecedent moisture in regulating water movement within the Andrews Forest. Both intra- and inter-catchment variability in $\delta^{18}O$ were greater during drier sampling periods (August) compared to wetter periods (May) (Figure 5). Though we also observed the largest difference in mean $\delta^{18}O$ between the two May samplings. During wet conditions, two competing factors contribute to our observations. Increased vertical connectivity within the subsurface leads to the introduction of

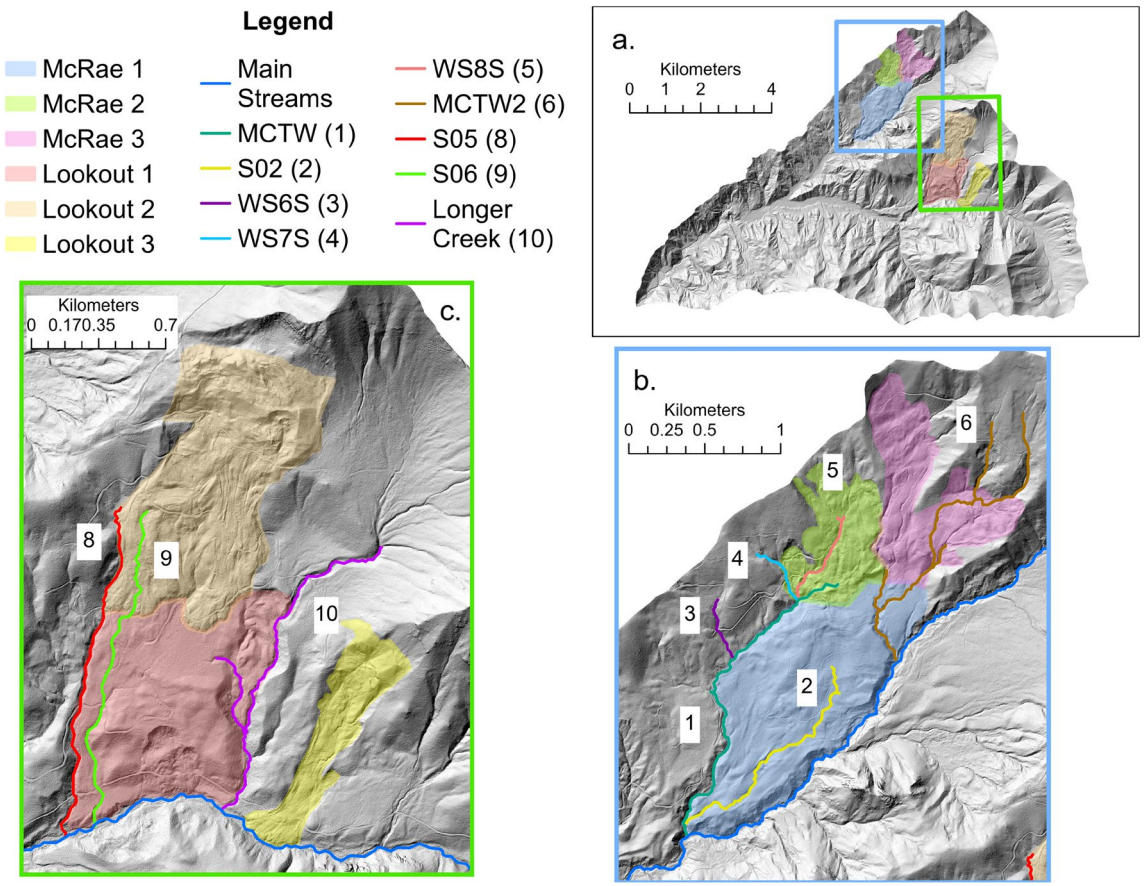

FIGURE 9 | (a) The landforms described in Table 2 are shown in (b) McRae Creek and (c) Upper Lookout drainages. Study streams that drain these landforms (nine out of twelve) are included (Figure 2).

TABLE 2 | Estimated deposit thickness for 6 landforms in the study region.

Landform ID	Streams draining landform	Characteristics**	Hydrologic observations	Deposit area (km^2)	Estimated thickness (m) [*n*]	Potential water storage (m^3)
Lookout 1	S05, S06	Deep-seated earthflows, majority are inactive, with some movement along the toe	Streamflow is intermittent, with streams emerging near the toe.	0.93	15.8 ± 1.6 [54]	3.7–5.9*10^6
Lookout 2	S05, S06	Deep-seated earthflow with active movement	Streamflow is intermittent, with streams emerging near the toe.	0.98	11.1 ± 0.8 [39]	2.7–4.4*10^6
Lookout 3	NA	Deep-seated earthflow with active movement	Streamflow is intermittent.	0.25	5.1 ± 0.9 [17]	3.2–5.1*10^5
McRae 1	S02, MCTW	Inactive landslide deposits	Streamflow is intermittent, with poorly defined channels. Pools and braiding streams are common.	1.29	23.5 ± 2.3 [59]	7.6–12*10^6
McRae 2	MCTW, WS8S, WS7S	Inactive landslide deposits of various sizes	Streamflow is intermittent, though perennial flows are present near the toe.	0.40	4.2 ± 0.6 [10]	4.2–6.7*10^5
McRae 3	MCTW2	Inactive landslide deposits of various sizes	Streamflow is intermittent, though perennial flows are present near the toe.	0.59	7.3 ± 0.7 [23]	1.1–1.7*10^6

Note: The landforms are split between the Lookout and McRae Creek valleys and are described in terms of their activity and mass movement characteristics. Thickness values were estimated using measurements of incision along stream channels and ± values represent standard error. *n*: Number of measurements used to estimate deposit thickness.

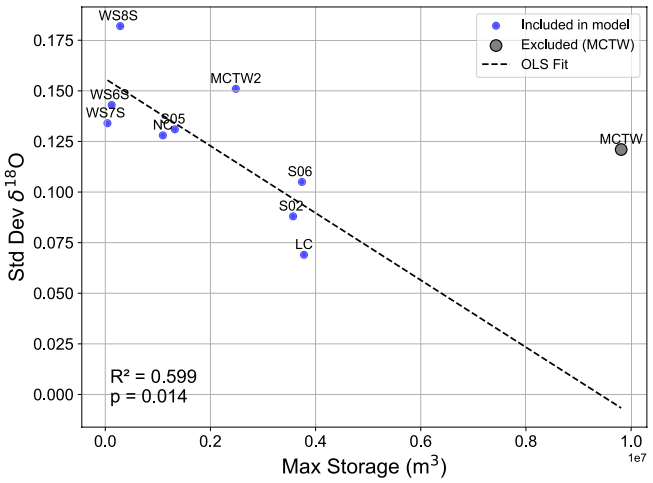

FIGURE 10 | Relationship between the standard deviation in $\delta^{18}O$ (‰) and catchment storage in landslide deposits for earthflow-dominated catchments. MCTW was excluded from the SLR because it is a large outlier in terms of catchment storage.

TABLE 3 | Regression statistics for model of standard deviation in $\delta^{18}O$ (‰) for earthflow-dominated catchments, predicted based on maximum catchment storage in landslide deposits (m^3).

Covariate	*b* (SE)	CI 95%	*p*	RMSE
Intercept	0.1560 (0.011)	[0.127, 0.185]		
Max storage	$-1.66*10^{-8}$ ($5.13*10^{-9}$)	[$-2.87*10^{-8}$, $-4.45*10^{-9}$]	0.014	0.0203

a well-mixed water source across catchments, leading to less intra-stream variability in $\delta^{18}O$. However, annual variability in climatic conditions and the resulting influence on mean $\delta^{18}O$ in annual precipitation plays a large role in determining the mean $\delta^{18}O$ across the site. As a result, wet season $\delta^{18}O$ can vary significantly in time, but we also observe less spatial variability between catchments. Alternatively, during dry conditions, vertical connectivity decreases and intra-stream variability in $\delta^{18}O$ increases as local variations in subsurface structure dictate where groundwater–surface water interactions occur. These patterns reflect changes in hydrologic connectivity, which alters the sources of surface water recharge under varying moisture conditions. Previous research has emphasised the critical role of antecedent moisture in shaping hydrologic connectivity across spatial scales (McGuire and McDonnell 2010; James and Roulet 2009; Jencso and McGlynn 2011).

These results have implications for understanding catchment responses to climate change, as dry conditions limit hydrologic connectivity to varying degrees across study streams. In the Andrews Forest, transit times are shorter and less variable across catchments during low-moisture conditions, reflecting the effects of reduced connectivity between surface and groundwater (Segura 2021). In contrast, during wet conditions, catchment characteristics and lithology strongly influence hydrologic variability (McGuire et al. 2005; Segura et al. 2019). These findings align with broader studies of mountainous catchments that emphasise the pivotal role of climate and wetness states in shaping hydrologic responses (Brooks et al. 2012, 2025; Heidbüchel et al. 2013; Hrachowitz et al. 2009; Seeger and Weiler 2014). Although our study does not measure the same hydrologic indices, it reflects a similar reality. For many study streams, temporal trends in $\delta^{18}O$ suggest that during wet conditions, hydrologic connectivity between surface water and groundwater sources increases. During dry conditions, connectivity decreases. However, access to groundwater remains in discrete points along the stream network. As the landscape dries, these inflows become increasingly important for generating streamflow and they dominate the $\delta^{18}O$ signal. In some streams (Cold Creek, Longer Creek, S02 and S06), though, the variability in $\delta^{18}O$ across sampling periods, even during dry conditions, was minimal. This indicates that these systems maintain relatively consistent groundwater connectivity under all conditions. The catchment areas of S06 and S02 drain 88%–99% landslide terrain, suggesting that some streams draining a high proportion of landslide deposits have strong, consistent hydrologic connectivity. However, most catchments in landslide terrain (WS6S, WS7S, WS8S, S05, NC, MCTW and MCTW2) exhibit contrasting results with high temporal variability in $\delta^{18}O$ that likely reflects varying connectivity through time and potentially different subsurface structure between deposits.

4.2 | Landscape Control on Spatial Variability in Groundwater Movement and Connectivity

By comparing deviations from expected $\delta^{18}O$ values (Figure 4) with spatial patterns of landslide deposits, we identified subsurface inter-catchment flow paths. Previous work in the volcanic and sedimentary landscapes of Oregon has demonstrated that water can travel considerable distances through highly permeable bedrock, especially in the High Cascades (Jefferson et al. 2006). Similarly, Nickolas et al. (2017) found that permeable bedrock in the Oregon Coast Range supports inter-catchment water movement from windward to leeward slopes. Other studies have emphasised how landforms such as alluvial fans, talus fields, and glacial moraines influence water storage and flow paths (Johnson, Christensen, et al. 2024; Liu et al. 2004; Gordon et al. 2015). Building on this work, we examine the role of landslide deposits in mediating interannual water storage and release (Swanson and Swanston 1977). Our results suggest that in volcanic terrain, deep flow paths allow upslope catchments to lose water, which then recharges downslope streams—highlighting the importance of subsurface hydrologic connectivity in small catchments.

In the McRae Creek drainage, where landslide deposits of varying size and depth are widespread (Figure 1c), isotopic evidence supports the presence of subsurface water transfer between headwater catchments. High $\delta^{18}O$ values in MCTW2 and WS8S, and lower-than-expected values in S02 (Figure 4), suggest that precipitation and snowmelt entering high-elevation deposits flow through thick (5–10 m) unconsolidated material before emerging as surface water downstream. MCTW2 and WS8S drain areas where 47%–49% of the landscape is underlain by landslide deposits. These deposits converge at a flatter bench where S02 (McRae 1) is located (Figure 9b). The $\delta^{18}O$ depletion in S02 indicates that a significant portion of its streamflow likely originates from outside the immediate catchment. The porosity

of the deposits—driven by high gravel content (25%–80%)—likely facilitates preferential flow (Dyrness 1969), consistent with recent findings linking gravel content to increased subsurface transport (Zhang et al. 2024). A similar process may explain the isotopic patterns in WS6S, where minimal change in $\delta^{18}O$ along the stream (Figure 6), coupled with a significant drop in values at the outlet in August 2021, the driest survey, points to sustained subsurface inflow from high elevations, which travel through landslide deposits on the slope. In contrast, WS7S—which lacks upper-elevation landslide deposits—shows $\delta^{18}O$ values that closely match expectations based on elevation (Figure 4), further supporting a geomorphic control on connectivity.

In the Upper Lookout Creek drainage, isotopic analysis reveals contrasting groundwater dynamics in S05 and S06, shaped by deep-seated earthflows. The $\delta^{18}O$ values are consistent in S06 along its profile, indicating strong and continuous groundwater input, particularly from landslide deposits at Lookout 2 (Figure 9c). In contrast, the values of $\delta^{18}O$ are lower at S05, illustrating a shift toward values near its outlet that match those of S06 in both August surveys (Figure 6), suggesting localised groundwater inflow where the landscape flattens into a bench at Lookout 1 (Figure 9c). Temporal analysis further supports these differences: S06 maintains stable $\delta^{18}O$ values across seasons, while S05 exhibits high groundwater input at a single point during dry periods and a more variable isotopic signature during wet periods, driven by recent recharge and increased vertical connectivity. These differences may stem from stream position relative to the earthflow. S06 flows through the centre of thick landslide deposits, capturing more subsurface drainage, whereas S05 skirts the margin, potentially limiting its connection to the primary groundwater storage zone.

Elsewhere, isotopic signatures continue to reveal subsurface processes. Cold Creek, for instance, shows depleted $\delta^{18}O$ values (Figure 5) suggestive of recharge from a high-elevation deep groundwater reservoir within porous lava flows along the upper ridge (Figure 1b). This pattern aligns with recent evidence of significant water storage in high-elevation lava flows of the High Cascades (Karlstrom et al. 2025). The findings of this study, though in a different landscape, support past hypotheses that the porous lava capping Cold Creek and the surrounding areas are supplying large amounts of snowmelt to the catchment. In contrast, Longer Creek shows minimal deviation from expected values (Figure 4), implying that water sources are primarily local. Despite both being groundwater-dominated streams, isotopic evidence suggests Longer Creek benefits from well-mixed recharge from both landslide deposits and porous lava bedrock, explaining the stable isotope ratios observed throughout the stream (Ortega et al. 2025).

4.3 | Hydrologic Implications of Streamflow Regimes and Patterns of Intermittent Flow

A snapshot of summer discharge at the Andrews Forest reveals highly variable streamflow generation mechanisms across the site. Higher unit discharge in culverts within the Lookout Creek drainage suggests stronger groundwater influence during baseflow conditions compared to the McRae Creek drainage (Figure 9a). In particular, Longer and Cold Creeks had significantly higher discharge than all other sites, confirming their role as spring-fed systems that sustain Lookout Creek baseflow (Segura et al. 2019; Ortega et al. 2025). Precipitation is higher in Upper Lookout compared to McRae, with total precipitation being highest along the ridges near Cold Creek (Daly 2015). This difference in precipitation explains some of the variability in unit discharge.

In S05, increasing specific discharge and isotopic variability downstream indicate greater groundwater input in lower reaches, with S05 eventually reflecting the same water source as S06. Culverts along S06 had significantly higher unit discharge than S05 and most other sites measured (Figure 8a). A small drainage near the top of S06 (C4) had a unit discharge similar to Cold Creek. Despite draining a very small surface area, we hypothesise that the active earthflow in this landscape provides flow path connectivity from the surrounding landscape to this point in the stream network. In Nostoc Creek, downstream increases in discharge correspond with a higher percentage of landslide deposits (21%–30%) and tributaries originating in old slides to the north. Although more culverts were flowing in Upper Lookout than McRae, most were concentrated on three perennial streams (Nostoc, S05, S06), intersected by several roads. Nonetheless, perennial stream persistence was higher in Upper Lookout, where the landscape is more heavily glaciated and the landslides are currently active (Swanson and Swanston 1977).

In contrast, McRae Creek's dry culverts suggest a dominance of intermittent streams (Figure 8), despite contributing 35%–75% of Lookout Creek's flow during winter months (Ortega et al. 2025). Isotopic data suggest this flow moves through deep subsurface pathways in extensive landslide deposits, bypassing smaller channels. Even where water was present, unit discharge in McRae's tributaries remained low compared to other sites (Figure 8). McRae Creek drainages tend to be smaller than those along Upper Lookout, likely due to a lack of glaciation and significant fluvial erosion. Indeed, our analysis showed that these smaller drainages were more likely to be dry than larger ones (Figure S6). The slumpier, less weathered landscape, which is made up of a mosaic of landslide deposits, means there is more subsurface storage potential, and therefore less likelihood of water reaching the surface. As hydrologic connectivity in the vertical dimension decreases as the climate transitions from wet to dry, these small reaches in landslide terrain lose access to stored water and run dry.

4.4 | Landform Evolution and Water Storage in the Andrews Forest

The results of this study suggest that landslide deposits and active earthflows can play a large role in subsurface water dynamics, as well as surface–groundwater interactions. Isotopic analysis indicates that these deposits may promote inter-catchment subsurface flow through which high elevation water can emerge in lower elevation streams. Additionally, deposits act as storage units, regulating vertical connectivity between streams and deeper groundwater. Groundwater movement through these deposits appears to be linked to their volume and position in the

landscape. Deposits on steep terrain appear to absorb water inputs and transmit them downslope until slope becomes gentler or an impermeable clay layer is encountered (Pyles et al. 1987), allowing water to emerge as streamflow. While these flow paths are most active during wet conditions, water from storage units continues to be important for streamflow generation during dry conditions. This could point to a mechanistic understanding of how sustained streamflow generation from interbasin flow paths persists during drought conditions in some catchments (Fan 2019; Wang et al. 2022). A conceptual figure of this process is shown in Figure 11. This figure illustrates the capacity for landslide deposits to allow for a complex series of inter- and intra-catchment flow paths during wet conditions. These flow paths move underneath topographic barriers and build up storage units in the deposits. During dry conditions, these flow paths stop conveying water and some sections of streamflow dry up, while others maintain streamflow via the exfiltration of water stored in the deposits during the wet season.

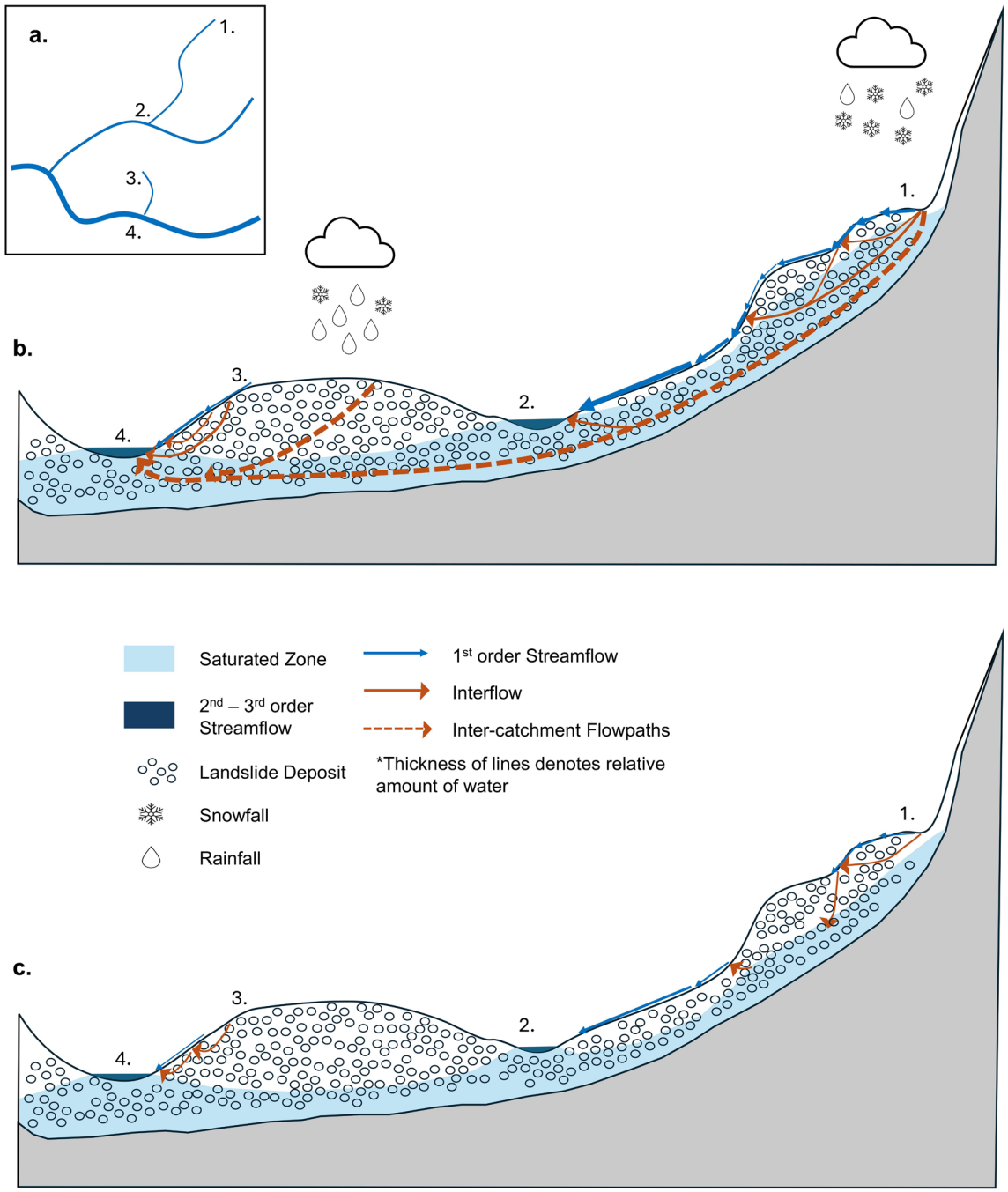

FIGURE 11 | Conceptual diagram of subsurface water dynamics in a landscape underlain by landslide deposits. (a) Plan view map of the catchment. (b) During wet conditions, high connectivity results in significant inter-catchment flow. High elevation water recharges storage in landslide deposits downslope. (c) During dry conditions, inter-catchment flow paths become disconnected as connectivity decreases. Localised storage in deposits can continue to support streamflow in 1st–3rd order streams. Thicker landslide deposits lead to increased streamflow intermittency, especially in 1st order streams.

The estimated storage potential of six different deposit landforms (Figure 9) represents a hypothetical maximum and the potential hydrologic importance of these landforms. Linear regression results indicate that storage in deposits is a significant predictor of isotopic variability. We found that increased storage leads to decreased isotopic variability and therefore more consistent hydrologic connectivity in both space and time. These results point to the role of landslide deposits in storing and releasing water to surface streamflow at inter-annual timescales.

In several landforms, including Lookout 1, 2, and 3, signs of recent earth movement—such as tipped trees, displaced roads, and open ground cracks—suggest that subsurface and surface water flow paths may be actively shifting over decadal timescales. These dynamics appear to influence the hydrologic function of the deposits, with younger or actively moving landforms potentially exhibiting different water storage and transmission behaviour than older, more stable ones. We speculate that these functions may also evolve over time, as active periods disrupt drainage patterns and inactive periods allow weathering and subsurface flow to reshape internal structure, but we lack the data to disentangle these conjectures. Additionally, thick, unconsolidated deposits can intermittently absorb stream water, contributing to disconnected or ephemeral stream reaches, particularly in small headwater systems. This highlights the potential for landslide age and activity to influence both surface stream intermittency and longer-term groundwater recharge patterns.

5 | Conclusion

This study highlights the critical role of antecedent moisture in regulating hydrologic connectivity within the Andrews Forest. Seasonal variations in $\delta^{18}O$ demonstrate that moisture conditions strongly influence both intra- and inter-catchment variability in water sources. During dry conditions, hydrologic disconnection from more ephemeral groundwater sources leads to greater spatial heterogeneity in isotopic composition. Wet conditions, on the other hand, promote greater connectivity throughout the landscape and isotopic homogenisation between catchments within a given year. However, inter-annual variations in precipitation vapour sources and evaporative fluxes can lead to large differences in overall isotopic composition of streamflow between years. These findings underscore the importance of antecedent moisture in shaping hydrologic responses, with potential implications for understanding catchment dynamics under future climate variability.

Additionally, landslide deposits and geology exert strong control on groundwater movement and connectivity. Evidence of inter-catchment subsurface flow in the McRae Creek and Upper Lookout Creek drainages suggests that landslide deposits, permeable bedrock, and earthflows facilitate complex water movement beyond topographically defined catchment boundaries. Streams draining landslide-affected terrain exhibit variable connectivity depending on moisture conditions, with some maintaining deep groundwater inputs during dry periods that are critical to flow throughout the larger basin. These findings align with prior research indicating that colluvial deposits and mass movement landforms can store and release water over extended timescales, influencing hydrologic connectivity across watersheds.

The implications of this work extend beyond the Andrews Forest, contributing to a broader understanding of hydrologic connectivity in mountainous catchments. The geomorphic and geologic conditions observed across the three geomorphic process domains in the Andrews Forest are representative of the Western Cascades and other mountainous terrains, suggesting that these results have relevance across other regions. This study highlights the hydrologic significance of landslide terrain, emphasising the need to incorporate landslide features into hydrologic models. Future work should focus on scaling this research to quantify the effects of colluvial terrain on catchment water budgets. Efforts to characterise landslide deposits using LiDAR have been attempted, with methods such as the Contour Connection Method finding success (Leshchinsky et al. 2015). We hope to utilise techniques such as these to investigate the hydrologic implications of landslide deposits across larger spatial scales in the Western Cascades and other mountainous systems.

Acknowledgements

The authors acknowledge the National Science Foundation (NSF) award no. EAR-1943574, LTER8DEB-2025755. We would like to thank members of the Segura research group for assistance in collecting precipitation and streamflow samples, Mark Schulze, Greg Downing, and Greg Cohn for assistance collecting precipitation samples, and Julia Jones, Daniele Penna, and Pamela Sullivan for helpful discussions. Streamflow and climate data were provided by the H.J. Andrews Experimental Forest and Long-Term Ecological Research (LTER), administered cooperatively by Oregon State University, the USDA Forest Service Pacific Northwest Research Station, and the Willamette National Forest. This material is based upon work supported by the National Science Foundation under the grant LTER8 DEB-2025755. Mention of trade names or commercial products does not constitute endorsement or recommendations for use.

Funding

This work was supported by the National Science Foundation grants EAR-1943574 and LTER8 DEB-2025755.

Data Availability Statement

Streamflow and climate data were provided by the HJ Andrews Experimental Forest and Long-Term Ecological Research (LTER) program, administered cooperatively by the USDA Forest Service Pacific Northwest Research Station, Oregon State University, and the Willamette National Forest. This material is based upon work supported by the National Science Foundation under the LTER8 DEB–2025755 (2020–2026).

References

Asano, Y., M. Kawasaki, T. Saito, et al. 2020. "An Increase in Specific Discharge With Catchment Area Implies That Bedrock Infiltration Feeds Large Rather Than Small Mountain Headwater Streams." *Water Resources Research* 56, no. 9: e2019WR025658. https://doi.org/10.1029/2019WR025658.

Benettin, P., N. B. Rodriguez, M. Sprenger, et al. 2022. "Transit Time Estimation in Catchments: Recent Developments and Future Directions." *Water Resources Research* 58, no. 11: e2022WR033096. https://doi.org/10.1029/2022WR033096.

Bowen, G. J., Z. Cai, R. P. Fiorella, and A. L. Putman. 2019. "Isotopes in the Water Cycle: Regional- to Global-Scale Patterns and Applications." *Annual Review of Earth and Planetary Sciences* 47, no. 1: 453–479. https://doi.org/10.1146/annurev-earth-053018-060220.

Bracken, L. J., and J. Croke. 2007. "The Concept of Hydrological Connectivity and Its Contribution to Understanding Runoff-Dominated Geomorphic Systems." *Hydrological Processes* 21, no. 13: 1749–1763. https://doi.org/10.1002/hyp.6313.

Bracken, L. J., J. Wainwright, G. A. Ali, et al. 2013. "Concepts of Hydrological Connectivity: Research Approaches, Pathways and Future Agendas." *Earth-Science Reviews* 119, no. April: 17–34. https://doi.org/10.1016/j.earscirev.2013.02.001.

Brooks, J. R., H. M. Johnson, K. Johnson, et al. 2025. "Inferring Snowpack Contributions and the Mean Elevation of Source Water to Streamflow in the Willamette River, Oregon Using Water Stable Isotopes." *Hydrological Processes* 39, no. 5: e70136. https://doi.org/10.1002/hyp.70136.

Brooks, J. R., P. J. Wigington Jr., D. L. Phillips, R. Comeleo, and R. Coulombe. 2012. "Willamette River Basin Surface Water Isoscape (δ18O and δ2H): Temporal Changes of Source Water Within the River." *Ecosphere* 3, no. 5: 1–21. https://doi.org/10.1890/ES11-00338.1.

Buchanan, B. P., M. Fleming, R. L. Schneider, et al. 2014. "Evaluating Topographic Wetness Indices Across Central New York Agricultural Landscapes." *Hydrology and Earth System Sciences* 18, no. 8: 3279–3299. https://doi.org/10.5194/hess-18-3279-2014.

Burns, W. J., and I. P. Madin. 2009. "Protocol for Inventory Mapping of Landslide Deposits From Light Detection and Ranging (Lidar) Imagery." DOGAMI Special Paper. 42.

Craig, H. 1961. "Isotopic Variations in Meteoric Waters." *Science* 133, no. 3465: 1702–1703. https://doi.org/10.1126/science.133.3465.1702.

Daly, C. 2015. "Average Monthly and Annual Precipitation Spatial Grids." (1971-2000 and 1980-1989), Andrews Experimental Forest. Long-Term Ecological Research. Forest Science Data Bank, Corvallis, OR. http://andlter.forestry.oregonstate.edu/data/abstract.aspx?dbcode=MS027. https://doi.org/10.6073/pasta/772a54d148ad9d1e291e4a951fd43cc20.

Daly, C., and J. Rothacher. 2019. "Precipitation Measurements From Historic and Current Standard, Storage and Recording Tain Gauges at the Andrews Experimental Forest, 1951 to Present." *Long-Term Ecological Research*. Forest Science Data Bank.

Daly, C., M. Schulze, and W. McKee. 2024. "Meteorological Data From Benchmark Stations at the HJ Andrews Experimental Forest, 1957 to Present." Long-Term Ecological Research. Forest Science Data Bank, Corvallis, OR. http://andlter.forestry.oregonstate.edu/data/abstract.aspx?dbcode=MS001. https://doi.org/10.6073/pasta/c021a2ebf1f91adf0ba3b5e53189c84f.

Dyrness, C. T. 1969. *Hydrologic Properties of Soils on Three Small Watersheds in the Western Cascades of Oregon*. Res. Note PNW-111, 17. U.S. Department of Agriculture, Forest Service, Pacific Northwest Forest and Range Experiment Station.

Fan, Y. 2019. "Are Catchments Leaky?" *WIREs Water* 6, no. 6: e1386. https://doi.org/10.1002/wat2.1386.

Finn, D. S., N. Bonada, C. Múrria, and J. M. Hughes. 2011. "Small but Mighty: Headwaters Are Vital to Stream Network Biodiversity at Two Levels of Organization." *Journal of the North American Benthological Society* 30, no. 4: 963–980. https://doi.org/10.1899/11-012.1.

Freeman, M. C., C. M. Pringle, and C. R. Jackson. 2007. "Hydrologic Connectivity and the Contribution of Stream Headwaters to Ecological Integrity at Regional Scales." *JAWRA Journal of the American Water Resources Association* 43, no. 1: 5–14. https://doi.org/10.1111/j.1752-1688.2007.00002.x.

Gao, M., X. Chen, J. Wang, C. Soulsby, and Q. Cheng. 2021. "Climate and Landscape Controls on Spatio-Temporal Patterns of Stream Water Stable Isotopes in a Large Glacierized Mountain Basin on the Tibetan Plateau." *Science of the Total Environment* 771: 144799. https://doi.org/10.1016/j.scitotenv.2020.144799.

Golden, H. E., J. R. Christensen, H. K. McMillan, et al. 2025. "Advancing the Science of Headwater Streamflow for Global Water Protection." *Nature Water* 3, no. 1: 16–26. https://doi.org/10.1038/s44221-024-00351-1.

Gómez, D., E. F. García, and E. Aristizábal. 2023. "Spatial and Temporal Landslide Distributions Using Global and Open Landslide Databases." *Natural Hazards* 117, no. 1: 25–55. https://doi.org/10.1007/s11069-023-05848-8.

Goodman, A. C., C. Segura, J. A. Jones, and F. J. Swanson. 2022. "Seventy Years of Watershed Response to Floods and Changing Forestry Practices in Western Oregon, USA." *Earth Surface Processes and Landforms* 48, no. 6: 1103–1118. https://doi.org/10.1002/esp.5537.

Gordon, R. P., L. K. Lautz, J. M. McKenzie, B. G. Mark, D. Chavez, and M. Baraer. 2015. "Sources and Pathways of Stream Generation in Tropical Proglacial Valleys of the Cordillera Blanca, Peru." *Journal of Hydrology* 522: 628–644. https://doi.org/10.1016/j.jhydrol.2015.01.013.

Gröning, M., H. O. Lutz, Z. Roller-Lutz, M. Kralik, L. Gourcy, and L. Pöltenstein. 2012. "A Simple Rain Collector Preventing Water re-Evaporation Dedicated for δ18O and δ2H Analysis of Cumulative Precipitation Samples." *Journal of Hydrology* 448: 195–200. https://doi.org/10.1016/j.jhydrol.2012.04.041.

Harr, R. D. 1976. "Hydrology of Small Forest Streams in Western Oregon." USDA Forest Service general technical Report. PNW-55.

Hawk, G., and C. T. Dyrness. 1972. "Vegetation and Soils of Watersheds 2 and 3, H.J. Andrews Experimental Forest." Seattle: University of Washington; Coniferous For. Biome Internal Rep. 49. 48.

Heidbüchel, I., P. A. Troch, and S. W. Lyon. 2013. "Separating Physical and Meteorological Controls of Variable Transit Times in Zero-Order Catchments." *Water Resources Research* 49, no. 11: 7644–7657. https://doi.org/10.1002/2012WR013149.

Hopkinson, C., M. Hayashi, and D. Peddle. 2009. "Comparing Alpine Watershed Attributes From LiDAR, Photogrammetric, and Contour-Based Digital Elevation Models." *Hydrological Processes* 23, no. 3: 451–463. https://doi.org/10.1002/hyp.7155.

Hrachowitz, M., C. Soulsby, D. Tetzlaff, J. J. C. Dawson, and I. A. Malcolm. 2009. "Regionalization of Transit Time Estimates in Montane Catchments by Integrating Landscape Controls." *Water Resources Research* 45, no. 5: 2008WR007496. https://doi.org/10.1029/2008WR007496.

James, A. L., and N. T. Roulet. 2009. "Antecedent Moisture Conditions and Catchment Morphology as Controls on Spatial Patterns of Runoff Generation in Small Forest Catchments." *Journal of Hydrology* 377, no. 3–4: 351–366. https://doi.org/10.1016/j.jhydrol.2009.08.039.

Jasechko, S. 2019. "Global Isotope Hydrogeology—Review." *Reviews of Geophysics* 57, no. 3: 835–965. https://doi.org/10.1029/2018RG000627.

Jefferson, A., G. Grant, and T. Rose. 2006. "Influence of Volcanic History on Groundwater Patterns on the West Slope of the Oregon High Cascades: Volcanic History Influences Groundwater." *Water Resources Research* 42, no. 12: W12411. https://doi.org/10.1029/2005WR004812.

Jencso, K. G., and B. L. McGlynn. 2011. "Hierarchical Controls on Runoff Generation: Topographically Driven Hydrologic Connectivity, Geology, and Vegetation." *Water Resources Research* 47, no. 11: 2011WR010666. https://doi.org/10.1029/2011WR010666.

Jennings, K., and J. A. Jones. 2015. "Precipitation-Snowmelt Timing and Snowmelt Augmentation of Large Peak Flow Events, Western Cascades, Oregon." *Water Resources Research* 51, no. 9: 7649–7661. https://doi.org/10.1002/2014WR016877.

Johnson, K., J. N. Christensen, W. Payton Gardner, et al. 2024. "Shifting Groundwater Fluxes in Bedrock Fractures: Evidence From Stream

Water Radon and Water Isotopes." *Journal of Hydrology* 635, no. May: 131202. https://doi.org/10.1016/j.jhydrol.2024.131202.

Johnson, S., S. Wondzell, and J. Rothacher. 2024. "Stream Discharge in Gaged Watersheds at the HJ Andrews Experimental Forest, 1949 to Present." Long-Term Ecological Research. Forest Science Data Bank, Corvallis, OR. http://andlter.forestry.oregonstate.edu/data/abstract.aspx?dbcode=HF004. https://doi.org/10.6073/pasta/ba33b8509dfd018f39f39f40d9f6dd7b.

Jones, J. A., and R. M. Perkins. 2010. "Extreme Flood Sensitivity to Snow and Forest Harvest, Western Cascades, Oregon, United States." *Water Resources Research* 46, no. 12: 2009WR008632. https://doi.org/10.1029/2009WR008632.

Kalra, A., T. C. Piechota, R. Davies, and G. A. Tootle. 2008. "Changes in U.S. Streamflow and Western U.S. Snowpack." *Journal of Hydrologic Engineering* 13, no. 3: 156–163. https://doi.org/10.1061/(ASCE)1084-0699(2008)13:3(156).

Karlstrom, L., N. Klema, G. E. Grant, et al. 2025. "State Shifts in the Deep Critical Zone Drive Landscape Evolution in Volcanic Terrains." *Proceedings of the National Academy of Sciences* 122, no. 3: e2415155122. https://doi.org/10.1073/pnas.2415155122.

Keller, C. K., G. Van Der Kamp, and J. A. Cherry. 1988. "Hydrogeology of Two Saskatchewan Tills, I. Fractures, Bulk Permeability, and Spatial Variability of Downward Flow." *Journal of Hydrology* 101, no. June: 97–121. https://doi.org/10.1016/0022-1694(88)90030-3.

Leshchinsky, B. A., M. J. Olsen, and B. F. Tanyu. 2015. "Contour Connection Method for Automated Identification and Classification of Landslide Deposits." *Computers & Geosciences* 74: 27–38. https://doi.org/10.1016/j.cageo.2014.10.007.

Liu, F., M. W. Williams, and N. Caine. 2004. "Source Waters and Flow Paths in an Alpine Catchment, Colorado Front Range, United States." *Water Resources Research* 40, no. 9: 2004WR003076. https://doi.org/10.1029/2004WR003076.

Lyon, S. W., M. Nathanson, A. Spans, et al. 2012. "Specific Discharge Variability in a Boreal Landscape." *Water Resources Research* 48, no. 8: 2011WR011073. https://doi.org/10.1029/2011WR011073.

Malet, J.-P., O. Maquaire, and T. van Asch. 2004. "Hydrological Behaviour of Earthflows Developed in Clay-Shales: Investigation, Concept and Modelling." In *The Occurrence and Mechanisms of Flows in Natural Slopes and Earthfills*, edited by L. Picarelli, 175–193. Patron Editore. https://hal.science/hal-01124437.

McGuire, K. J., J. J. McDonnell, M. Weiler, et al. 2005. "The Role of Topography on Catchment-Scale Water Residence Time." *Water Resources Research* 41, no. 5: W05002. https://doi.org/10.1029/2004WR003657.

McGuire, K. J., and J. J. McDonnell. 2010. "Hydrological Connectivity of Hillslopes and Streams: Characteristic Time Scales and Nonlinearities." *Water Resources Research* 46, no. 10: W10543. https://doi.org/10.1029/2010WR009341.

McGuire, K. J., and J. J. McDonnell. 2015. "Tracer Advances in Catchment Hydrology." *Hydrological Processes* 29, no. 25: 5135–5138. https://doi.org/10.1002/hyp.10740.

Mote, P. W., S. Li, D. P. Lettenmaier, M. Xiao, and R. Engel. 2018. "Dramatic Declines in Snowpack in the Western US." *Npj Climate and Atmospheric Science* 1, no. 1: 2. https://doi.org/10.1038/s41612-018-0012-1.

Mueller, M. H., R. Weingartner, and C. Alewell. 2013. "Importance of Vegetation, Topography and Flow Paths for Water Transit Times of Base Flow in Alpine Headwater Catchments." *Hydrology and Earth System Sciences* 17, no. 4: 1661–1679. https://doi.org/10.5194/hess-17-1661-2013.

Nereson, A. L., S. Davila Olivera, and N. J. Finnegan. 2018. "Field and Remote-Sensing Evidence for Hydro-Mechanical Isolation of a Long-Lived Earthflow in Central California." *Geophysical Research Letters* 45, no. 18: 9672–9680. https://doi.org/10.1029/2018GL079430.

Nickolas, L. B., C. Segura, and J. R. Brooks. 2017. "The Influence of Lithology on Surface Water Sources." *Hydrological Processes* 31, no. 10: 1913–1925. https://doi.org/10.1002/hyp.11156.

Nippgen, F., B. L. McGlynn, and R. E. Emanuel. 2015. "The Spatial and Temporal Evolution of Contributing Areas." *Water Resources Research* 51, no. 6: 4550–4573. https://doi.org/10.1002/2014WR016719.

Nippgen, F., B. L. McGlynn, L. A. Marshall, and R. E. Emanuel. 2011. "Landscape Structure and Climate Influences on Hydrologic Response." *Water Resources Research* 47, no. 12: 2011WR011161. https://doi.org/10.1029/2011WR011161.

OCM Partners. 2025. "USFS 2020 Lidar: Wallowa-Whitman National Forest." https://www.fisheries.noaa.gov/inport/item/69262.

Ortega, J., C. Segura, J. R. Brooks, and P. L. Sullivan. 2025. "Insights Into Heterogeneous Streamflow Generation Processes and Water Contribution in Forested Headwaters." *Hydrological Processes* 39: e70241.

Payn, R. A., M. N. Gooseff, B. L. McGlynn, K. E. Bencala, and S. M. Wondzell. 2012. "Exploring Changes in the Spatial Distribution of Stream Baseflow Generation During a Seasonal Recession." *Water Resources Research* 48, no. 4: 2011WR011552. https://doi.org/10.1029/2011WR011552.

Penna, D., H. J. van Meerveld, O. Oliviero, et al. 2015. "Seasonal Changes in Runoff Generation in a Small Forested Mountain Catchment." *Hydrological Processes* 29, no. 8: 2027–2042. https://doi.org/10.1002/hyp.10347.

Pfister, L., N. Martínez-Carreras, C. Hissler, et al. 2017. "Bedrock Geology Controls on Catchment Storage, Mixing, and Release: A Comparative Analysis of 16 Nested Catchments." *Hydrological Processes* 31, no. 10: 1828–1845. https://doi.org/10.1002/hyp.11134.

Pringle, C. M. 2001. "Hydrologic Connectivity and the Management of Biological Reserves: A Global Perspective." *Ecological Applications* 11, no. 4: 981–998. https://doi.org/10.1890/1051-0761(2001)011[0981:HCATMO]2.0.CO;2.

Pyles, M. R., K. Mills, and G. Saunders. 1987. "Mechanics and Stability of the Lookout Creek Earth Flow." *Environmental & Engineering Geoscience* 24, no. 2: 267–280. https://doi.org/10.2113/gseegeosci.xxiv.2.267.

Richardson, J. S. 2020. "Headwater Streams." In *Encyclopedia of the World's Biomes*, 371–378. Elsevier. https://doi.org/10.1016/B978-0-12-409548-9.11957-8.

Rock, L., and B. Mayer. 2007. "Isotope Hydrology of the Oldman River Basin, Southern Alberta, Canada." *Hydrological Processes* 21, no. 24: 3301–3315. https://doi.org/10.1002/hyp.6545.

Rothacher, J., C. T. Dyrness, and R. L. Fredriksen. 1967. *Hydrologic and Related Characteristics of Three Small Watersheds in the Oregon Cascades*, 54. U.S. Department of Agriculture, Forest Service, Pacific Northwest Forest and Range Experiment Station.

Seeger, S., and M. Weiler. 2014. "Reevaluation of Transit Time Distributions, Mean Transit Times and Their Relation to Catchment Topography." *Hydrology and Earth System Sciences* 18, no. 12: 4751–4771. https://doi.org/10.5194/hess-18-4751-2014.

Segura, C. 2021. "Snow Drought Reduces Water Transit Times in Headwater Streams." *Hydrological Processes* 35, no. 12: e14437. https://doi.org/10.1002/hyp.14437.

Segura, C., D. Noone, D. Warren, J. A. Jones, J. Tenny, and L. M. Ganio. 2019. "Climate, Landforms, and Geology Affect Baseflow Sources in a Mountain Catchment." *Water Resources Research* 55, no. 7: 5238–5254. https://doi.org/10.1029/2018WR023551.

Segura, C., Z. Perry, and J. Ortega. 2025. "Water Stable Isotopes for Streams and Precipitation Samples in the HJ Andrews Experimental

Forest and Mary's River Watershed, 2014–2023." Long-Term Ecological Research. Forest Science Data Bank, Corvallis, OR. http://andlter.forestry.oregonstate.edu/data/abstract.aspx?dbcode=HF028. https://doi.org/10.6073/pasta/f7bfbab3132ac23002d5df6e837a9d0e.

Shaman, J., M. Stieglitz, and D. Burns. 2004. "Are Big Basins Just the Sum of Small Catchments?" *Hydrological Processes* 18, no. 16: 3195–3206. https://doi.org/10.1002/hyp.5739.

Siirila-Woodburn, E. R., A. M. Rhoades, B. J. Hatchett, et al. 2021. "A Low-To-No Snow Future and Its Impacts on Water Resources in the Western United States." *Nature Reviews Earth and Environment* 2: 800–819. https://doi.org/10.1038/s43017-021-00219-y.

Soulsby, C., C. Birkel, J. Geris, J. Dick, C. Tunaley, and D. Tetzlaff. 2015. "Stream Water Age Distributions Controlled by Storage Dynamics and Nonlinear Hydrologic Connectivity: Modeling With High-Resolution Isotope Data: Stream Water Age Controlled by Storage and Connectivity." *Water Resources Research* 51, no. 9: 7759–7776. https://doi.org/10.1002/2015WR017888.

Swanson, F. J. 2013. "Upper Blue River Geology Clipped to the Andrews Experimental Forest, 1991 Ver 4." Environmental Data Initiative. https://doi.org/10.6073/pasta/1c428e8798a2f3975f202636d3ad6139.

Swanson, F. J., and M. E. James. 1975. *Geology and Geomorphology of the H.J. Andrews Experimental Forest, Western Cascades, Oregon*, 14. U.S. Department of Agriculture, Forest Service, Pacific Northwest Forest and Range Experiment Station Res. Pap. PNW-188.

Swanson, F. J., and D. N. Swanston. 1977. "Complex Mass-Movement Terrains in the Western Cascade Range, Oregon." In *Landslides. Reviews in Engineering Geology*, edited by D. R. Coates, vol. 3, 113–124. Geological Society of America. https://doi.org/10.1130/REG3-p113.

Tetzlaff, D., J. Seibert, K. J. McGuire, et al. 2009. "How Does Landscape Structure Influence Catchment Transit Time Across Different Geomorphic Provinces?" *Hydrological Processes* 23, no. 6: 945–953. https://doi.org/10.1002/hyp.7240.

Vano, J. A., B. Nijssen, and D. P. Lettenmaier. 2015. "Seasonal Hydrologic Responses to Climate Change in the Pacific Northwest." *Water Resources Research* 51, no. 4: 1959–1976. https://doi.org/10.1002/2014WR015909.

Varnes, D. J. 1978. "Slope Movement Types and Processes." In *Landslides, Analysis and Control, Special Report 176: Transportation Research Board*, edited by R. L. Schuster and R. J. Krizek, 11–33. National Academy of Sciences.

Walker, G. W., and N. S. MacLeod. 1991. "Geologic Map of Oregon." U. S. Geological Survey, Scale 1:500,000, 2 sheets, U. S. Geological Survey.

Wang, C., J. D. Gomez-Velez, and J. L. Wilson. 2022. "Dynamic Coevolution of Baseflow and Multiscale Groundwater Flow System During Prolonged Droughts." *Journal of Hydrology* 609: 127657. https://doi.org/10.1016/j.jhydrol.2022.127657.

Weekes, A. A., C. E. Torgersen, D. R. Montgomery, A. Woodward, and S. M. Bolton. 2014. "Hydrologic Response to Valley-Scale Structure in Alpine Headwaters." *Hydrological Processes* 29: 356–372. https://doi.org/10.1002/hyp.10141.

Xiao, D., Y. Shi, S. L. Brantley, et al. 2019. "Streamflow Generation From Catchments of Contrasting Lithologies: The Role of Soil Properties, Topography, and Catchment Size." *Water Resources Research* 55, no. 11: 9234–9257. https://doi.org/10.1029/2018WR023736.

Zhang, L., Z. Zhan, Z. Zhang, et al. 2024. "Morphological and Structural Characteristics of Preferential Flow and Its Influencing Factors on Colluvial Deposits of Benggang." *Earth Surface Processes and Landforms* 49, no. 9: 2870–2883. https://doi.org/10.1002/esp.5863.

Zhang, Z., X. Chen, Q. Cheng, and C. Soulsby. 2019. "Storage Dynamics, Hydrological Connectivity and Flux Ages in a Karst Catchment: Conceptual Modelling Using Stable Isotopes." *Hydrology and Earth System Sciences* 23, no. 1: 51–71. https://doi.org/10.5194/hess-23-51-2019.

Supporting Information

Additional supporting information can be found online in the Supporting Information section. **Table S1:** Catchment scale characteristics of study streams. All data was derived from a 1-m resolution DEM* with values rounded to the nearest meter. **Figure S1:** (a) Mean snow water equivalent (SWE) from three meteorological stations: VANMET, UPLMET, CENMET (Figure 1, Daly and Rothacher 2019). (b) Mean cumulative flow from Lookout Creek USGS gauge No. 14161500. (c) Mean cumulative precipitation from two meteorological stations (CENMET, UPLMET). (d) Soil moisture content (SMC) from CENMET (average of sensors at 4 soil depths: 10, 20, 50 and 100 cm). The dashed lines in each plot represent the water year mean values 2003–2023. Each plot shows the sampling dates with a unique icon—these dates are the final day for each respective sampling. **Figure S2:** Relationship between $\delta^{18}O$ (‰) and $\delta^{2}H$ (‰) using all stream data after evaporated samples were removed (identified as samples with d-excess of less than 8). **Figure S3:** Depth of incision measurements. (a) A large mass-movement deposit in the McRae Creek drainage (b) Red circles represent locations where depth of incision was measured. (c) A cross section of the valley at a single measurement point highlights how the measurements were taken to estimate deposit depth. The cross section from A–B in b is translated to an elevation profile in (c). **Figure S4:** Individual cross section measurement locations of stream channel incision and deposit toe thickness used to estimate deposit thickness. Summary statistics for estimates of landslide deposit depths in Table S6. **Table S2:** Results of statistical comparison of mean $\delta^{18}O$ (‰) between synoptic campaigns. Overall means $\delta^{18}O$ (‰) were calculated for each campaign and comparisons were made using Kruskal-Wallis Test ($H = 184.62$, $p = 7.58*10^{-39}$). Pairwise comparisons were completed using the Wilcoxon rank-sum test ($\alpha = 0.95$). **Table S3:** Mean $\delta^{18}O$ (‰) for each site, during each synoptic sampling campaign, with corresponding standard error. Number in parentheses corresponds to the sample size. **Table S4:** Summary of overall mean $\delta^{18}O$ (‰) values for each site with standard error. Overall mean $\delta^{18}O$ was calculated using all available data from synoptic sampling campaigns. Sample count is shown in parentheses next to mean $\delta^{18}O$. **Figure S5:** Heat map showing the results of the statistical comparison of mean $\delta^{18}O$ (‰) between study catchments. This analysis was completed using the overall mean $\delta^{18}O$ for each catchment over the entire study. Kruskal–Wallis Test was used to determine if there is statistical differences between at least one pair of means ($H = 857.20$, $p = 7.64 \times 10^{-175}$). Pairwise comparisons were made using Dunn's Test with Bonferroni correction and the results of this are shown in the heat map ($\alpha = 0.95$). **Table S5:** Slopes (‰/100 m) for the relationship between elevation (m) and $\delta^{18}O$ (‰) for each site, during each sampling campaign, as well as the mean slope and standard deviation of the slope. **Figure S6:** Statistical comparison of drainage areas between stream crossing culverts that were observed to be flowing vs. those observed to be dry. Statistical comparison was made using the Wilcox Rank-Sum test (p-value = 0.0013). **Table S6:** Summary of statistics for landform thickness measurements. Values were calculated using individual cross section measurements from Table S6. **Table S7:** Estimates of maximum storage within landslide deposits for each study catchment.